Structures 25 (2020) 743–759

Contents lists available at ScienceDirect

Structures

journal homepage: www.elsevier.com/locate/structures

Optimization of partially connected composite beams using nonlinear programming

Amilton R. Silva[a], Francisco de A. das Neves[a,*], João B.M. Sousa Junior[b]

[a] Department of Civil Engineering, Federal University of Ouro Preto, Ouro Preto, Brazil
[b] Department of Civil Engineering, Federal University of Ceará, Fortaleza, Brazil

ARTICLE INFO

Keywords:
Optimization
Composite beams
Interface elements
Simplex
Sequential linear programming

ABSTRACT

Due to concrete being consistently used in the filling of prefabricated linear steel structural floor slabs, the practice of constructing steel-concrete composite structures is becoming more and more popular. The joint action of the two materials is generally ensured by mechanical connectors that considerably increase the performance of the composite element structure. For a majority of practical cases, these elements are formed by a concrete slab connected to I-shaped steel beams. In this study, models of finite elements for the steel-concrete composite beams with partial interaction are optimized using the sequential linear programming algorithm. The design variables are considered with two approaches: in the first, only the parameters that define the cross section of the steel "I" profile vary, while in the second, besides the aforementioned parameters that define the cross section of the "I" profile, also considered are those that define the concrete section. In addition, the optimum distribution of the shear connectors along the composite beam are verified; in other words, the longitudinal rigidity of the deformable connection is considered to be a design variable. The design constraints are those defined in standard specifications referring to the dimensioning of concrete, steel and composite steel-concrete structures, as well as the side constraints with respect to the parameters defining the cross section and the step-size for the non-linear optimization algorithm. The results for the composite beam optimization problems are presented taking into consideration different boundary conditions. For a given optimized project, the analysis of the results is done regarding the influence of the constraints on the optimization process, the graph of the load-slip curve along the composite beam, and the values obtained for the design variables.

1. Introduction

For a majority of the steel constructions, the composite beam solution is adopted in order to make use of the concrete slab height, which overlays the steel beam, forming a composite beam with a structural behavior that is superior to the steel beam. This gain in the structural behavior of the composite element, together with the growing usage of steel structures in Brazil's civil construction industry has generated a relative increase in the use of this constructive technique. This type of solution is also used when long spans need to be conquered, as in the case of bridges and industrial sheds. Nie et al. [1] cites these cases as advantages of the composite beams in relation to the simple beams due to the fact that there is a high ratio for span versus beam depth, less deformation, and a high fundamental vibration frequency. For motives that are generally practical or economic, the interaction between the different structural elements that compose the composite element, promoted by the connectors, is partial, or in other words, a relative displacement between the different elements occurs on the interface of the contact between them, which is generally called sliding in the interface in literature.

Despite the fact of many journal papers treat of the optimization on steel, concrete or composite steel-concrete structures, only a few of them address the problem of optimization of composite beams, especially on partially connected composite beams. Aiming to provide an overview about this subject, a succinct review follows. Eskandari and Korouzhdeh [2] presented a method described as simple and efficient exact solution that can be applied in practical engineering problems instead of predictions model such as artificial neural network and genetic algorithm, aiming to be applied for practical designs. García-Segura et al. [3] proposed a new hybrid method combining simulated annealing with glowworm swarm optimization (SAGSO) algorithms to optimize a concrete I-beam. Kravanja and et al. [4] presented a comparative study of design, resistance and economical properties of a composite floor system, composed from a concrete slab and steel I

* Corresponding author.
E-mail addresses: amilton@ufop.edu.br (A.R. Silva), fassis@ufop.edu.br (F.d.A. das Neves), joaobatistasousajr@hotmail.com (J.B.M. Sousa).

https://doi.org/10.1016/j.istruc.2020.03.007
Received 20 August 2019; Received in revised form 23 February 2020; Accepted 2 March 2020
Available online 03 April 2020

sections based on the multi-parametric mixed-integer non-linear programming (MINLP) approach and Eurocode specifications. Papavasileiou and Charmpis [5] used a structural optimization framework for the seismic design of multi–storey composite buildings, based on Eurocodes 3 and 4, with steel HEB-columns fully encased in concrete, steel IPE-beams and steel L-bracings. A discrete Evolution Strategies algorithm and OpenSees software were utilized, respectively, to perform optimization and all structural analyses. Senouci and Mohammed [6] employed a genetic algorithm model for the cost optimization of composite beams based on the load and resistance factor design (LRFD) specifications of the AISC. The model formulation includes the cost of concrete, steel beam, and shear studs. Kaveh and Abadi [7] presented the cost optimization of a composite floor system, comprised of a reinforced concrete slab and steel I-beams, where the design constraints are implemented as in LRFD-AISC rules. Kaveh and Ahangaran [8] developed an economical social harmony search model to perform the discrete cost optimization of composite floors where design is based on AISC–LRFD specifications and plastic design concepts. Kravanja and Z˘ula [9] performed the problem of simultaneous cost, topology and standard cross-section optimization of single storey industrial steel building structures in accordance with Eurocode 3. The optimization is effectuated by the mixed-integer non-linear programming approach, MINLP. Munck et al. [10] developed a methodology to optimize hybrid composite-concrete beams, made out of multiple materials with very different cost/weight ratios, towards the two objectives of cost and mass, varying the geometry of the elements. An original methodology combining Non-dominated Sorting Genetic Algorithm (NSGA-II) and a *meta*-model is used to find all optimal solutions. A comparison between composite welded I beams and composite trusses with hollow sections were accomplished by Kravanja and Silih [11]. Composite I beams and composite trusses were designed in accordance with Eurocode 4 for the conditions of both ultimate and serviceability limit states. The optimization was performed by the Nonlinear Programming (NLP) and Mixed-Integer Nonlinear Programming approaches. Recently, Pedro et al. [12] developed an efficient two-stage optimization approach to the design of steel-concrete composite I-girder bridges. In the first step, a simplified structural model is employed aiming to locate the global optimum region and provide a starting point to the local search. Then, a finite element model (FEM) is used to refine and improve the optimization. The performance of five *meta*-heuristic algorithms for this specific problem was evaluated: Back-tracking Search Algorithm (BSA), Firefly Algorithm (FA), Genetic Algorithm (GA), Imperialist Competitive Algorithm (ICA) and Search Group Algorithm (SGA).

What it is common for all of these published works is that almost none of them approach the problem of optimization using a formulation taking into consideration partially connected composite beams. Thus, by combining the developed simplex algorithm, in a fashion to be applied for solving nonlinear optimization problem using the sequential linear programming, with that for the analysis of composite beams with deformable shear connection one gets a powerful and robust numerical tool for the optimization of beams with partial interaction.

The main objective of this study was to implement an optimization routine within a structural analysis program based on the finite element method (FEM). To simulate composite beam behavior with partial interaction, one-dimensioned beam elements are used to represent the behavior of the material above and below the sliding interface of the composite section and the interface elements to represent the sliding interface behavior. For design variables, different approaches are considered. In the first approach, the variables for the project considered are the dimensions of the steel I profile, along with those of the concrete slab and the reinforcing bars defined by the designer, according to Silva et al [13]. In the second approach, the dimension of the steel I profile, along with those of the concrete slab are considered as design variables. And finally, the rigidity of the deformable connection is considered to be a design variable. Through an iterative process that controls the step-size of each iteration, the nonlinear problem involving the variation of the composite beam's structural behavior in relationship with the project variables is approximated by a linear problem, which has its optimum point defined at each step when using the Simplex method.

This article is organized as follows: Section 2 presents the Simplex method for sequential linear programming that will be used in each step of the iterative process for the solution of a constrained linear problem; In the Section 3, a brief description of the finite element formulation employed to consider the shear deformable interface between the concrete and steel in composite beams is presented; Section 4 presents the constraints of the project for optimization of the composite beams with partial interaction, considering different objective functions and design variables; Section 5 presents the objective functions for the different problems approached in this study, as well as the standard Simplex form of these problems; Section 6 analyzes the different examples in order to illustrate the robustness of the method implemented in this study; and finally in Section 7 some conclusions are cited.

2. The Simplex method

The Simplex method was developed by Dantzig in the latter part of the 40′s and marks the beginning of the modern optimization era. Immediately following this development, the method was computerized and established itself as a powerful optimization tool for the fields of economy, administration and engineering. Briefly, the linear programming problem and the Simplex algorithm are presented as follow.

In linear programming, the objective function, as well as the constraints for equality and inequality, is linear. A set of variable points form a polyhedron that is convex and has its faces given by polygons. The linear programming is initiated and analyzed in its standard form.

$$\min c^T x \; subject \; to \; Ax = b, x \geq 0 \tag{1}$$

where **c** and **x** are vectors in $\Re^n$, **b** is a vector in $\Re^m$and **A** is the matrix *m* x *n*. All linear optimization problems with equality and inequality constraints can be easily placed in the standard format given by Eq. (1). For greater details as to how to do this for different forms of linear programming, refer to Nocedal and Wright [14]; Vanderplaats[15]; Haftka and Kamat [16].

Using the Lagrange method, problem (1) can be placed in the form expressed by Eq. (2), where the Lagrange multipliers are separated into a vector π of *m* order for equal constraints, and into vector **s** of *n* order for unequal constraints.

$$\Im(x,\pi,s) = c^T x - \pi^T(Ax - b) - s^T x \tag{2}$$

The linearity of problem (1) and its convexity ensure that if a feasible point $\mathbf{x}^*$ satisfies the first-order optimality condition of KKT (Karush, Kuhn and Tucker, see Bazaraa and Shetty [17]), given by Eq. (3), then this point becomes the optimum for problem (1).

$$A^T\pi + s = c \tag{3-a}$$

$$Ax = b \tag{3-b}$$

$$x \geq 0 \tag{3-c}$$

$$s \geq 0 \tag{3-d}$$

$$x_i s_i = 0,\ i = 1, 2, ..,n \tag{3-e}$$

If $\mathbf{x}^*$ satisfies the condition of (3-a), then

$$c^T x^* = (A^T\pi^* + s^*)^T x^* = (Ax^*)^T\pi^* + s^{*T}x^*$$

From condition (3-b), we have$Ax^* = b$, and from conditions (3-c), (3-d) and (3-e), we have; $s^{*T}x^* = 0$; thus $c^T x^* = b^T\pi^*$.

From the result of the previous paragraph, it is easy to see that whatever other feasible point $\bar{x}$, in other words, $A\bar{x} = b$and $\bar{x} \geq 0$, satisfies $c^T\bar{x} \geq c^T x^*$. This is because:

$$c^T\bar{x} = (A^T\pi^* + s^*)^T\bar{x} = b^T\pi^* + s^{*T}\bar{x}$$

as $b^T\pi^* = c^T x^*$, and from the conditions (3-c) and (3-e), we have

$s^{*T}\bar{x} \geq 0$, whereby $c^T\bar{x} \geq c^T x^*$. As such, the point $\bar{x}$ will be optimum if and only if $s^{*T}\bar{x} = 0$, which signifies that for the values of $s_i \geq 0$, it is necessary that $\bar{x}_i = 0$.

Considering that the matrix $\mathbf{A}_{mxn}$ has full row ranking, in other words, equal to m, and that we can define a subset $\beta(x)$ of the set with an index of {1, 2, ..,n} so that,

I. $\beta(x)$ contains exactly m indexes.
II. $i \in \beta(x)$ implies that $x_i = 0$.
III. The matrix $\mathbf{B}_{mxm}$, defined by $B = [A_i]_{i\in\beta(x)}$, is not singular where A_i is the ith column of **A**.

If all of the above conditions are satisfied for a design point x, than this point is said to be the basic feasible point. In its iterative process, the Simplex method generates a sequence of basic feasible points, stopping when these points satisfy the conditions given by Eq. (3-a)–(3-e), which will be the optimum point of the linear problem of Eq. (1). This point could be unique, or more vertices of the polyhedron. In the case that more than one vertex of the polyhedron is the optimum point, we have that whatever point on the straight line or plane that connects such vertices of the polyhedron will also be the optimum point.

The simplex iterations evolve by evaluating if a feasible point, which is a vertex of the polyhedron, satisfies the first-order optimality conditions of KKT. If satisfied, than such point will be the problem's solution point (1); to the contrary, a new basic feasible point, or in other words, another vertex of the polyhedron should be evaluated. This point is obtained by defining a new subset $\beta(x)$ of the set for the index {1, 2, ..,n}.

To understand which index in $\beta(x)$ should exit and which should enter to define another basic feasible point in a Simplex iteration, we define the subset $\eta(x)$ of the set with index {1, 2, ..,n}, as being the complement of $\beta(x)$. And in the same way that **B** was defined, we will define N as

$$N = [A_i]_{i\in\eta(x)}$$

We separated the vectors x, **s** and **c** in accordance with the subsets $\beta(x)$ and $\eta(x)$, which are now denoted by

$$x_B = [x_i]_{i\in\beta(x)}, x_N = [x_i]_{i\in\eta(x)},$$

$$s_B = [s_i]_{i\in\beta(x)}, s_N = [s_i]_{i\in\eta(x)},$$

$$c_B = [c_i]_{i\in\beta(x)} \; e \; c_N = [c_i]_{i\in\eta(x)}.$$

From condition (3-b), we have

$$Ax = Bx_B + Nx_N = b \tag{4}$$

Admitting$x_N = 0$, we have from Eq. (4), $x_B = B^{-1}b$. To satisfy the condition (3-e), we can set $s_B = 0$. From condition (3-a), we can define π and s_N, given by $B^T\pi = c_B$ and $N^T\pi + s_N = c_N$, so that,

$$\pi = B^{T-1}c_B \quad and \tag{5}$$

$$s_N = c_N - (B^{-1}N)^T c_B \tag{6}$$

If s_N, defined by Eq. (6), satisfies $s_{Ni} \geq 0$ for all $i \in \eta(x)$, then the basic feasible point evaluated is the solution of the problem of presented in Eq. (1). On the contrary, that is when one or more of the components of s_{Ni} are negative, then a new point should be evaluated. The index q in $\eta(x)$ that should be submitted to index p in $\beta(x)$ is such that $s_{Nq} < 0$, while the index p should be the smallest between:

$$\frac{x_{Bi}}{t_i} \tag{7}$$

for $t_i > 0$ and $i \in \beta(x)$, where $t = B^{-1}A_q$.

3. Finite element formulation: beam and interface element

In order to supply an idea of the finite element formulation employed to consider the shear deformable interface between the concrete and steel in composite beams is presented a summary of the equations in terms of the internal forces vector and the tangent stiffness matrix and figures to illustrate the deformations and degrees of freedom of beam and interface elements. For more details, the readers can see other works of the authors (Sousa and Silva [18], Sousa and Silva [19], Sousa et al. [20], Silva and Sousa [21], Sousa [22], Machado et al. [23]), where an numerical solution for the analysis of composite beams with deformable shear connection is developed and applied on different aspects. The solution treats with the development of a specific zero-thickness interface element to represent the behavior of the connection, associated with inelastic two-noded beam elements. The upper and lower parts of the composite beam may be of generic cross-section, and analytical integration of section forces and tangent moduli are employed, thus yielding a powerful and robust numerical tool for the analysis of beams with partial interaction (Sousa and Silva [18,19]).

In numerical modeling of the composite beam, the concrete slab and steel I beam is simulated by one-dimensional beam element, while the deformable shear connection by a one-dimensional interface element.

3.1. Euler-Bernoulli theory

3.1.1. Displacement equations

Assuming that the composite beam lies in the *xy* plane, the displacement field is given by (Fig. 1)

$$u_\alpha(x, y) = u_\alpha(x) - (y - y_\alpha)v'_\alpha(x) \tag{8}$$

$$v_\alpha(x, y) = v_\alpha(x) \tag{9}$$

where $\alpha = 1,\ldots,2$ represents the upper and the lower element, respectively, and y_α is the reference axis for each constituent element, which is usually taken at the centroid.

3.1.2. Interface sliding

The interface element to be used for the simulation of the deformable connection has two translational and one rotational displacement

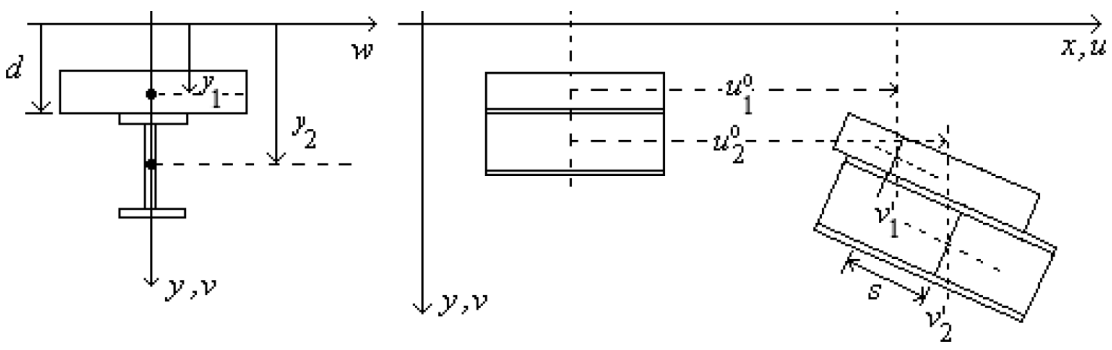

Fig. 1. Displacement field of composite beam.

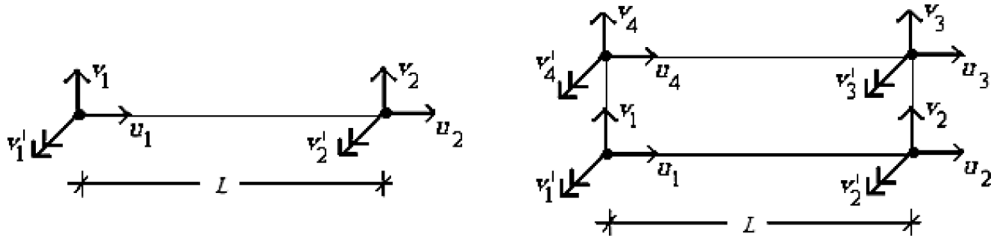

Fig. 2. Degrees of freedom for interface and beam element.

at each node, Fig. 2. The displacement field has for the tangential relative displacement

$$s(x) = u_2^0(x) - u_1^0(x) + (y_2 - d)v_2'(x) - (y_1 - d)v_1'(x) \tag{10}$$

3.1.3. Relative vertical displacement

and for the normal relative displacement

$$w(x) = v_2(x) - v_1(x) \tag{11}$$

Application of the principle of virtual work to the isolated beam and interface element leads, after some manipulations, to the equations of the internal force vector and the element tangent stiffness matrix.

3.1.4. Interface elements

From the internal virtual work expression one gets into a standard fashion the internal force vector. Related to this vector and Fig. 1, d, y_1 and y_2 are contact interface positions and reference axes of the upper and lower parts of the composite beam, respectively. Shear and normal forces along the contact interface are designated, respectively, by S_b and N_b. While Φ_u and Φ_v are, respectively, vectors containing the interpolation functions for axial and transverse displacements. For the four-node interface element associated with two-node beam elements, where a joint interpolation of transverse displacements and rotation is accomplished, there are linear interpolation functions for axial displacements and cubic for transverse displacements, so Φ_u it has two terms and Φ_v has four terms.

$$\mathrm{f_{int}} = \int_L \begin{Bmatrix} -S_b\Phi_u \\ (d-y_1)S_b\Phi_v' - N_b\Phi_v \\ S_b\Phi_u \\ (y_2-d)S_b\Phi_v' + N_b\Phi_v \end{Bmatrix} dx \tag{12}$$

The derivation of $\mathbf{f}_{\mathrm{int}}$ with respect to the nodal displacements ($\mathbf{q}$) gives the element tangent stiffness matrix

$$\mathrm{K}_T = \int_l \begin{Bmatrix} -\Phi_u\left(\frac{\partial S_b}{\partial \mathrm{q}}\right)^T \\ (d-y_1)\Phi_v'\left(\frac{\partial S_b}{\partial \mathrm{q}}\right)^T - \Phi_v\left(\frac{\partial N_b}{\partial \mathrm{q}}\right)^T \\ \Phi_u\left(\frac{\partial S_b}{\partial \mathrm{q}}\right)^T \\ (y_2-d)\Phi_v'\left(\frac{\partial S_b}{\partial \mathrm{q}}\right)^T + \Phi_v\left(\frac{\partial N_b}{\partial \mathrm{q}}\right)^T \end{Bmatrix} dx \tag{13}$$

3.1.5. Beam elements

The interface element developed in the work [18] may be associated to a two-noded beam-column element with displacement and rotational DOF. As the main concern there is the modeling of composite steel–concrete beams with interlayer slip, the elements implemented had cubic interpolation of transverse displacements and linear interpolation of axial displacements. By applying the same procedure used to the interface element, one gets the internal force vector, Eq. (14), and element tangent stiffness matrix, Eq. (15) for the beam element. In these equations, N and M are the normal and bending forces developed in the transverse section of the beam, respectively. As seen for the interface element, Φ_u and Φ_v are vectors containing the interpolation functions for axial and transverse displacements, respectively, and $\mathbf{q}$, the nodal displacements vector.

$$\mathrm{f_{int}} = \int_L \begin{Bmatrix} N\Phi_u' \\ -M\Phi_v'' \end{Bmatrix} dx \tag{14}$$

$$\mathrm{K}_T = \int_L \begin{bmatrix} \Phi_u'\left(\frac{\partial N}{\partial \mathrm{q}}\right)^T \\ -\Phi_v''\left(\frac{\partial M}{\partial \mathrm{q}}\right)^T \end{bmatrix} dx \tag{15}$$

4. Formulation of the constraints for composite beam analysis

For the problem analyzed in this study, we considered the safety criteria for: the concrete's maximum compressive stress, the maximum tensile stress of reinforcing bars in the concrete section, the maximum tensile stress in the steel profile, and maximum force on the connectors, as well as local buckling of the flanges and web of the steel profile and, as serviceability limit state criteria, the maximum deflection of the beam span is considered. These constraints are defined through the dimensioning criteria adopted by standards to ensure safety and utilization of the structure, such as NBR-6118 [24] for concrete and NBR 8800 [25] for steel and composite steel/concrete elements.

Besides the constraints cited in the previous paragraph, others in relation to the steel dimension profiles, concrete section dimensions, maximum and minimum spacing between the shear connectors, as well as the size of the iterative processing step should be considered.

More details in relation to the constraint expressions defined in the sub-items below can be obtained in the article of Silva et al. [13].

4.1. Stress on the concrete section and reinforcing bars

The composite section consists of a concrete slab with the reinforcement bars connected to a steel I profile. In the discretization of a problem for a partially interacting composite beam, the beam elements are used to simulate the behavior of the concrete sections and the steel profile. Thus, to determine the maximum compression stress on the concrete section, and the stresses on the reinforcing bars along the composite beam, all beam elements that represent the concrete section should be processed.

Assuming that there is a linear stress-strain relationship for the materials of the composite section, we have

$$\sigma(\xi, y) = E_c(u_0' - y\chi) = E_c[\varphi_u'^T \quad -y\varphi_v''^T]\mathrm{q} \tag{16}$$

In Eq. (16), E_c is the modulus for concrete deformation; φ_u and φ_v are form functions for the axial displacements (linear interpolation) and cross-sections/rotations (cubic interpolation), respectively, giving $\mathrm{q} = [u_1 \;\; u_2 \;\; v_1 \;\; \theta_1 \;\; v_2 \;\; \theta_2]$ as the vector of the nodal displacements of the beam element.

As in Eq. (16) φ_u' is the constant and φ_v'' is linear along the element, then $\sigma(\xi, y)$ is maximum and minimum at the element extremes, or:

$$\sigma(\xi = -1, y) = E_c[\varphi_u'^T(\xi = -1) \quad -y\varphi_v''^T(\xi = -1)]\mathrm{q} \tag{17}$$

and

$$\sigma(\xi = 1, y) = E_c[\varphi_u'^T(\xi = 1) \ -y\varphi_v''^T(\xi = 1)]q \tag{18}$$

It should be remembered that in Eqs. (17) and (18), the derivatives are related to the global variable x and the shape functions are defined in relationship to the local variable ξ of the element.

With h being the height of the concrete slab, $\sigma_1 = \sigma(\xi = -1, -h/2)$, $\sigma_2 = \sigma(\xi = -1, h/2)$, $\sigma_3 = \sigma(\xi = 1, -h/2)$ and $\sigma_4 = \sigma(\xi = 1, h/2)$, we can determine that:

$$\sigma_{1,\max} = \textit{the greatest value for } \sigma_j \text{with } j = 1, ..,4 \tag{19}$$

$$\sigma_{2,\min} = \textit{the least value for } \sigma_j \text{with } j = 1, ..,4 \tag{20}$$

For each stress defined in Equations (19) and (20) a stress on the other face of the rectangular concrete section is determined by $\sigma_{1,\min}$ and $\sigma_{2,\max}$. The maximum compression stress of the concrete (σ_c) of the analyzed element is given by $\sigma_{2,\min}$, if $\sigma_{2,\min} < 0$; to the contrary, the compression's stress is null. Meanwhile, the maximum compressive stress of the reinforcing bars (σ_{S_b}) is obtained in accordance with one of the three cases below, which are verified for each pair of stresses ($\sigma_{1,\max}$, $\sigma_{1,\min}$) and ($\sigma_{2,\max}$, $\sigma_{2,\min}$):

Case 1: $\sigma_{1,\max} > 0$ and $\sigma_{1,\min} < 0$.

From Fig. 3, we can determine:

$$h' = \frac{\sigma_{1,\max}}{\sigma_{1,\max} - \sigma_{1,\min}} h \tag{21}$$

Due to the linear physical condition of the problem analysis, the concrete section resists a traction force given by:

$$F_t = \frac{\sigma_{1,\max}}{2} h'b \tag{22}$$

In Eq. (22), b is the width of the rectangular concrete section. As the concrete's resistance to traction is ignored, the force given by Eq. (22) should be resisted by the reinforcing bars.

In Fig. 4, c is the cover of the reinforcing bars. From the equilibrium condition of the moments in relation to B, we have:

$$F_A = \frac{h - c - h'/3}{h - 2c} F_t \tag{23}$$

From the equilibrium condition of the horizontal forces, we have:

$$F_B = F_t - F_A \tag{24}$$

The stresses on the rebars due to the deformation of the section are given by:

$$\sigma_A = E_s \varepsilon_A \textit{ Where } \varepsilon_A = \frac{h' - c}{h'} \varepsilon_{1,\max} \textit{ and} \tag{25}$$

$$\sigma_B = E_s \varepsilon_B \textit{ Where } \varepsilon_B = \frac{h'' - c}{h''} \varepsilon_{1,\min} \tag{26}$$

In Eq. (26), $h'' = h - h'$, the maximum tensile stress on the reinforcing bars (σ_{S_b}) of the analyzed element is given by the greatest value between $\left|\frac{F_A}{A} + \sigma_A\right|$ and $\left|\frac{F_B}{A} + \sigma_B\right|$, where A is the area of the cross-section of the reinforcing bars.

Case 2: $\sigma_{1,\max} > 0$ and $\sigma_{1,\min} > 0$

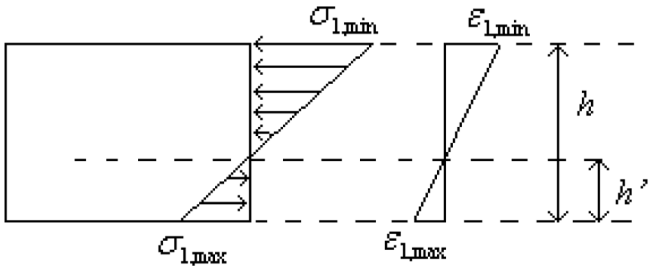

Fig. 3. Stresses acting on the concrete section.

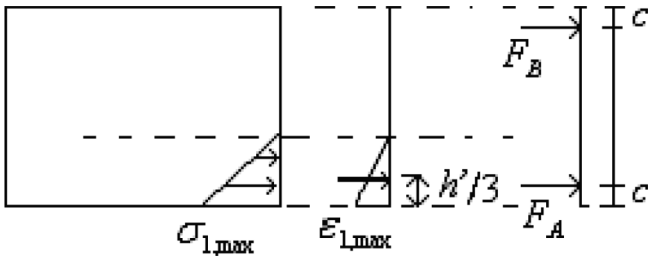

Fig. 4. Traction stress on the concrete section.

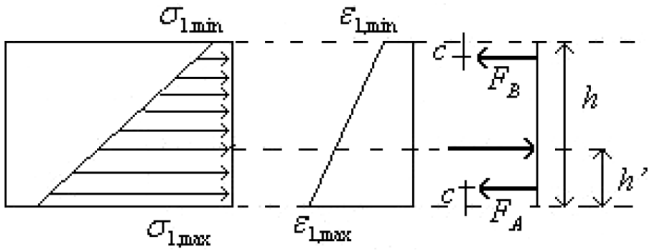

Fig. 5. Stresses acting on the concrete section.

As $\sigma_{1,\min} > 0$, then the whole concrete section is under traction, as shown in Fig. 5.

In Fig. 5, c is the cover of the reinforcing bars of the concrete section. This figure determines that:

$$h = \left(1 + \frac{\sigma_{1,\min}}{\sigma_{1,\max} + \sigma_{1,\min}}\right)\frac{h}{3} \tag{27}$$

The traction force acting on the concrete section is given by:

$$F_t = \frac{\sigma_{1,\max} + \sigma_{1,\min}}{2} hb \tag{28}$$

In Eq. (28), b is the width of the rectangular concrete section. As the concrete's resistance to traction is ignored, the force given by Eq. (28) should be resisted by the reinforcing bars.

From the equilibrium condition of the moments in relation to B, see Fig. 5, we have:

$$F_A = \frac{h - c - h'}{h - 2c} F_t \tag{29}$$

From the equilibrium condition of the horizontal forces, we have:

$$F_B = F_t - F_A \tag{30}$$

The stresses on the bars due to deformation of the section are given by:

$$\sigma_A = E_s \varepsilon_A \textit{ where } \varepsilon_A = (\varepsilon_{1,\min} - \varepsilon_{1,\max})\frac{c}{h} + \varepsilon_{1,\max} \textit{ and} \tag{31}$$

$$\sigma_B = E_s \varepsilon_B \textit{ where } \varepsilon_B = (\varepsilon_{1,\min} - \varepsilon_{1,\max})\frac{h - c}{h} + \varepsilon_{1,\max} \tag{32}$$

The maximum stress on the reinforcing bars (σ_{S_b}) in the analyzed element is given by the greater value between $\left|\frac{F_A}{A} + \sigma_A\right|$ and $\left|\frac{F_B}{A} + \sigma_B\right|$, where A is the area of the cross section of the reinforcing bars.

Case 3: $\sigma_{1,\max} < 0$ and thus $\sigma_{1,\min} < 0$

As $\sigma_{1,\max} < 0$, then the entire concrete section is compressed as shown in Fig. 6

As the section is entirely compressed, the acting stress on the bars depends only on the deformation of these, then:

$$\sigma_A = E_s \varepsilon_A \textit{ where } \varepsilon_A = (\varepsilon_{1,\min} - \varepsilon_{1,\max})\frac{c}{h} + \varepsilon_{1,\max} \textit{ and} \tag{33}$$

$$\sigma_B = E_s \varepsilon_B \textit{ where } \varepsilon_B = (\varepsilon_{1,\min} - \varepsilon_{1,\max})\frac{h - c}{h} + \varepsilon_{1,\max} \tag{34}$$

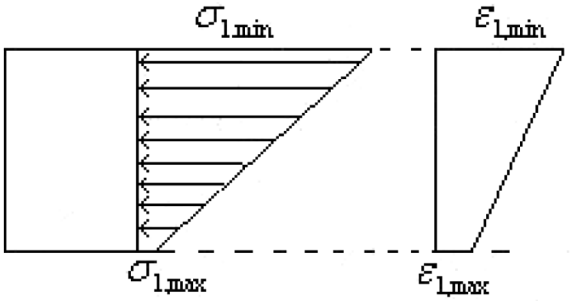

Fig. 6. Stresses acting on the concrete section.

The maximum stress on the reinforcing bars (σ_{S_b}) of the analyzed element is given by the greater value between $|\sigma_A|$and$|\sigma_B|$.

The stress resistance limit to the concrete compression ($\bar{\sigma_c}$) is given by $\bar{\sigma_c} = 0.85 f_{cd}$.

Herein, $f_{ck} = 30MPa$, $E_c = 0.85(5600\sqrt{f_{ck}})$ and $f_{cd} = f_{ck}/1.4$were adopted, while for the reinforcing bars, $E_S = 210000MPa$, $f_{yk} = 500MPa$ and $f_{yd} = f_{yk}/1.15$were used. Thus, the stress resistance limit for the compression or traction of the reinforcing bars ($\bar{\sigma_{S_b}}$) is given by:

$$\bar{\sigma_{S_b}} = f_{yd}$$

The equations for these two constraints are defined in the form presented below:

$C_1(\mathrm{x}) = \sigma_c - \bar{\sigma_c} \geq 0$ and

$$C_2(\mathrm{x}) = \bar{\sigma_{S_b}} - \sigma_{S_b} \geq 0$$

4.2. Stress on the steel section

In a manner similar to that which was obtained for the maximum compressive stress of the concrete section, we determine the maximum stress on the steel section (σ_S).

$$\sigma(\xi, y) = E_S(u_0' - y\chi) = E_S[\varphi_u'^T - y\varphi_v''^T]\mathrm{q} \tag{35}$$

In Eq. (35), E_S is the steel's deformation modulus and the rest is defined as in Eq. (16).

As in Eq. (35) φ_u' is constant and φ_v' is linear along the element, then $\sigma(\xi, y)$ is the maximum and minimum of the extremities of the element, so that:

$$\sigma(\xi = -1, y) = E_S[\varphi_u'^T(\xi = -1) - y\varphi_v''^T(\xi = -1)]\mathrm{q}\ \text{and} \tag{36}$$

$$\sigma(\xi = 1, y) = E_S[\varphi_u'^T(\xi = 1) - y\varphi_v''^T(\xi = 1)]\mathrm{q} \tag{37}$$

Remembering that in Eqs. (36) and (37), the derivatives are related to the variable x global and the shape functions are defined in relation to the local variable ξ of the element. With h being the total height of the steel I profile, $\sigma_1 = \sigma(\xi = -1, -h/2)$, $\sigma_2 = \sigma(\xi = -1, h/2)$, $\sigma_3 = \sigma(\xi = 1, -h/2)$ and $\sigma_4 = \sigma(\xi = 1, h/2)$, we determine:

$$\sigma_{\max} = \textit{the greatest between}\ \sigma_j \textit{com}\ j = 1, ..,4\ \textit{and} \tag{38}$$

$$\sigma_{\min} = \textit{the least between}\ \sigma_j \textit{com}\ j = 1, ..,4 \tag{39}$$

The maximum stress on the steel profile (σ_S) will be the greatest value between $|\sigma_{\max}|$ and $|\sigma_{\min}|$.

Herein, for the steel I profile, $E_S = 210000MPa$, $f_{yk} = 500MPa$ and $f_{yd} = f_{yk}/1.15$were adopted. Thus, the stress resistance limit for compression or traction for the profile ($\bar{\sigma_S}$) is given by $\bar{\sigma_S} = f_{yd}$.

The equation for this constraint is defined as given below:

$$C_3(\mathrm{x}) = \bar{\sigma_S} - \sigma_S \geq 0$$

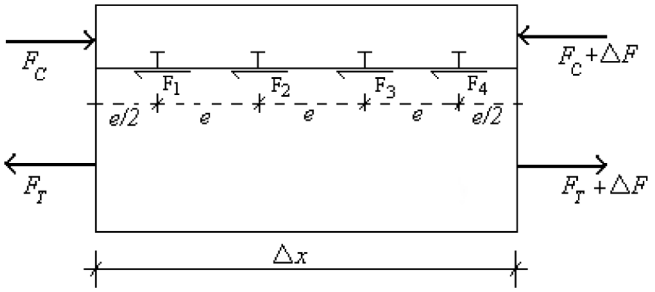

Fig. 7. Acting forces in a composite beam element.

4.3. Maximum force on the connectors

Fig. 7 displays a composite beam element and the resulting forces acting on it. When the horizontal forces are in equilibrium, we have:

$$\Delta F = \sum_{i=1}^{n} F_i \tag{40}$$

In Eq. (40), F_i represents the forces in each connector due to displacement s between the steel and concrete sections. According to Oehlers and Coughlan [26], a bolt connector has a linear behavior until 50% of its maximum force resistance. The same authors relate the connector's rigidity modulus with the maximum force it can resist ($F_{\max}$), the diameter of its base (d_c), and the concrete's resistance to compression that is involved (f_c), as shown in Eq. (41).

$$K_c = \frac{F_{\max}}{d_c(0.16 - 0.00172 f_c)} \tag{41}$$

In Eq. (41), the dimensions are in N and mm.$F_{\max} = 0.5A_{sh}\sqrt{f_c E_c}$, where A_{sh} is the area of the cross-section of the connector's base.

Assuming that the displacement is the same along the element in Fig. 7 and that the connectors are all the same, we have:

$$\Delta F = nK_c s \tag{42}$$

By defining $K = nK_c/\Delta x$ and substituting it in Eq. (42), we have:

$$\frac{\Delta F}{\Delta x} = Ks, \qquad or \tag{43}$$

for a small Δx, $F' = Ks$. Considering a constant spacing between the connectors along $\Delta x$with value e, we have $ne = \Delta x$, and as such:

$$K = K_c/e \tag{44}$$

The project for the revision of the standard NBR-8800 [25] limits the spacing between connectors as six times the diameter of the connector, and when adopting a connector diameter of 19 mm, we have $e_{\min} = 11.4$cm. After determiningK_c, using Eq. (41), we obtain from Eq. (44), the maximum rigidity allowed on the sliding interface. This rigidity was utilized in the numerical analysis of the composite beam.

The maximum force acting on a connector due to the deformation of the composite beam should be calculated at the level of the element through the integral equation $F' = Ks$, where the integration limits should be spaced according to the spacing between the connectors, being thus:

$$F_1 = \int_{-1}^{-1+e} Ksdx,\ F_2 = \int_{-1+e}^{-1+2e} Ksdx,\ F_n = \int_{1-e}^{1} Ksdx$$

The maximum acting force (F_s) will be the greatest value of$|F_1|$, $|F_2|$, …, $|F_n|$.

According to NBR-8800 [25] the maximum force resisted by a connector ($\bar{F_s}$) should be the least of the two values.

$$\bar{F_s} = \frac{0.5A_{cs}\sqrt{f_{ck}E_c}}{\gamma_{cs}} \tag{45}$$

$$\bar{F_s} = \frac{A_{cs} f_u}{\gamma_{cs}} \tag{46}$$

For Eqs. (45) and (46), A_{cs} is the area of the cross-section of the connector, f_u is the rupture resistance stress of the connector, and $\gamma_{cs} = 1.25$.

The equation for this constraint is defined as below:

$$C_4(\mathrm{x}) = \bar{F_s} - F_s \geq 0$$

4.4. Maximum deflection

The equation for the transverse displacement in an element is given by:

$$v(\xi) = [0^T \quad \varphi_v^T]\mathrm{q} \tag{47}$$

where $\mathrm{q} = [u_1 \quad u_2 \quad v_1 \quad \theta_1 \quad v_2 \quad \theta_2]$ is the vector of the nodal displacements of the beam element, and φ_v is the vector of the shape functions for the transverse displacements/rotations. As cubic interpolation is adopted for these displacements, we have the maximum displacement ($v_{\max}$) being in one of the extremities of the element ($\xi = -1$ or $\xi = 1$), or at some point within the element where the derivative is null ($v'(\xi) = 0$), which could be two, one or none.

For this study, we have adopted a transverse limit deflection ($\bar{v}$) of $L/350$, where L is the length of the beam's span.

The equation for this constraint is then defined as written below:

$$C_5(\mathrm{x}) = \bar{v} - v_{\max} \geq 0$$

4.5. Local buckling of the steel profile

According to NBR-8800 [25] the local buckling effects can be ignored when determining the cross-sections resistance forces for the case of I profiles with a web slenderness ratio less than:

$$\lambda_w = 3.76\sqrt{\frac{E_s}{f_y}}$$

And with a flange slenderness ratio less than:

$$\lambda_f = 0.38\sqrt{\frac{E_s}{f_y}}$$

Being that the flange slenderness ratio is given by the relationship $b_f/(2t_f)$, where t_f is the thickness of the flange and b_f is it width, and the web slenderness ratio is given by b_w/t_w, where t_w is the thickness of the web and b_w is its height.

The constraint equations are then defined as below:

$$C_6(\mathrm{x}) = t_f - \frac{1}{2\lambda_f} b_f \geq 0$$

$$C_7(\mathrm{x}) = t_w - \frac{1}{\lambda_w} b_w \geq 0$$

4.6. Profile and concrete section dimensions

Constraints regarding the total height of the steel I profile are adopted herein, along with the minimum and maximum dimensions for the web and flanges and concrete section's height and width.

Define $\bar{h}$ as the height limit of profile I, $\bar{t_i}$ and $\bar{t_s}$ respectively as the thickest and thinnest thickness possible for the web and flanges, $\bar{b_i}$ and $\bar{b_s}$ as the narrowest and widest widths possible of the web and flanges, $\bar{h_i}$ and $\bar{h_s}$ as the smallest and greatest height possible for the concrete section, and also $\bar{l_i}$ and $\bar{l_s}$ as the narrowest and widest width possible for the concrete section. These constraints can then be written as presented below:

$$C_8(\mathrm{x}) = \bar{h} - (2t_f + b_w) \geq 0$$

$$C_9(\mathrm{x}) = t_w - \bar{t_i} \geq 0$$

$$C_{10}(\mathrm{x}) = \bar{t_s} - t_w \geq 0$$

$$C_{11}(\mathrm{x}) = t_f - \bar{t_i} \geq 0$$

$$C_{12}(\mathrm{x}) = \bar{t_s} - t_f \geq 0$$

$$C_{13}(\mathrm{x}) = b_f - \bar{b_i} \geq 0$$

$$C_{14}(\mathrm{x}) = \bar{b_s} - b_f \geq 0$$

$$C_{15}(\mathrm{x}) = b_w - \bar{b_i} \geq 0$$

$$C_{16}(\mathrm{x}) = \bar{b_s} - b_w \geq 0$$

$$C_{17}(\mathrm{x}) = h_c - \bar{h_i} \geq 0$$

$$C_{18}(\mathrm{x}) = \bar{h_s} - h_c \geq 0$$

$$C_{19}(\mathrm{x}) = l_c - \bar{l_i} \geq 0$$

$$C_{20}(\mathrm{x}) = \bar{l_s} - l_c \geq 0$$

4.7. Spacing between the connectors (longitudinal stiffness of the connection)

For an approach considering the longitudinal rigidity as a variable of the project, the spacing limit between shear connectors should be considered as a constraint, or in other words, the longitudinal rigidity of the connection should have upper and lower limits. Considering $\bar{K_i}$ and $\bar{K_s}$ as the rigidity limits of the connection, we have the equations below for these constraints:

$$C_{21}(\mathrm{x}) = \bar{K_s} - K_j) \geq 0$$

$$C_{22}(\mathrm{x}) = K_j - \bar{K_i} \geq 0$$

In the above equations, K_j refers to the longitudinal rigidity of a connection simulated by an interface element, the index j refers to a stretch of the composite beam that has constant spacing between connector, or in other words, the same longitudinal rigidity of the connection. The number of stretches of the composite beam with different spacing between the connectors can be any amount, remembering that this would influence the number of design variables and constraints.

4.8. Iterative step size

As the Simplex method is linear, the problem of determining the optimum steel I profile dimensions of a composite beam should be linearized, truncating its expansion in the first term to the Taylor series.

Adopting the step size limit as value $\bar{d}$ and calling f the function that need to be minimized, we have:

$$f(\mathrm{x}_k + \mathrm{d}) = f(\mathrm{x}_k) + \nabla^T f_k \mathrm{d}$$

And thus, $\nabla^T f_k \ \mathrm{d} \leq |\bar{d}|$ limits the step size.

5. The objective function and standard form of the simplex method

5.1. Optimization of the steel I profile

In this first approach, we intend to determine the steel profile dimensions of a composite concrete-steel beam with partial interaction, so that the cross-section area of the steel beam is the minimum possible. Therefore, in accordance with Fig. 8, the objective function can be defined in the following manner:

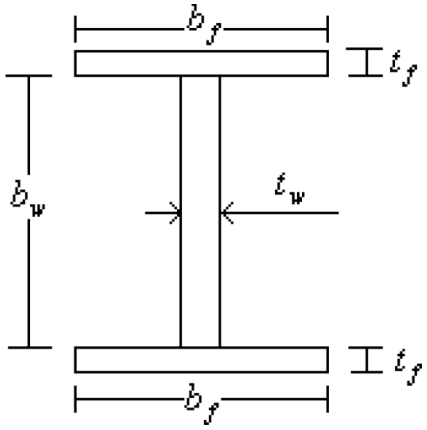

Fig. 8. Steel profile.

$$f(\mathrm{x}) = 2b_f t_f + b_w t_w \tag{48}$$

Where the vector x is given by $\mathrm{x}= [b_f \;\; t_f \;\; t_w \;\; b_w]$.

The optimization of the problem is given by:

$$\min_{\mathrm{x}} f(\mathrm{x}) \; subject \; to \; C_i(\mathrm{x}) \geq 0 \tag{49}$$

Substituting the objective function and the constraints by their expansion from the truncated Taylor series in the first term, we have the linear optimization problem:

$$\min_{\mathrm{d}} \nabla^T f_k \mathrm{d} \; subject \; to \; \nabla^T C_{i,j} \; \mathrm{d} \geq \; - C_i(\mathrm{x}_k) \; and \; \nabla^T f_k \; \mathrm{d} \leq |\bar{d}| \tag{50}$$

In the above equation, i varies from 1 until the number of constraints, j varies from 1 until the number of design variables, and **d** refers to the step of the incremental process for the solution of the nonlinear problem.

Placing the linear problem of Eq. (50) in the standard Simplex method form, we have:

$$\min_{\mathrm{d}^*} [\nabla^T f_k \;\; -\nabla^T f_k \;\; 0_{1\times 18}] \mathrm{d}*$$

Subject to

$$\begin{bmatrix} \nabla^T C_{i,k} & -\nabla^T C_{i,k} & -\mathbf{I}_{16\mathrm{x}16} & 0 & 0 \\ \nabla^T f_k & -\nabla^T f_k & \mathbf{0}_{1\times 16} & -1 & 0 \\ -\nabla^T f_k & \nabla^T f_k & \mathbf{0}_{1\times 16} & 0 & -1 \end{bmatrix} \mathbf{d}^* = \begin{bmatrix} -C_i(\mathrm{x}_k) \\ -\bar{d} \\ -\bar{d} \end{bmatrix} \tag{51}$$

In the equation above, $\mathrm{d}^* = [\mathrm{d}^{+T} \;\; \mathrm{d}^{-T} \;\; \mathrm{u}^T \;\; \mathrm{w}^T]^T$, where d^+ and d^- are two vectors with 4 components (number of design variables), **u** is a vector with 16 components (number of constraints), **w** is a vector with 2 components (referring to the step size constraint), $\mathbf{I}_{16\mathrm{x}16}$ is an identity matrix of order 16, and $\mathbf{0}_{1\mathrm{x}16}$ is a matrix line with 16 columns of null elements. For greater details as to how to arrive at this standard form, consult Vanderplaats [15]; Haftka and Kamat [16].

The derivatives in relation to the objective function and the constraints of $C_i(\mathrm{x})$ with $i = 5,\ldots,16$ are obtained in an analytic manner by deriving these equations in relation to $x_0 = b_f$, $x_1 = t_f$, $x_2 = t_w$ and $x_3 = b_w$. While the derivatives $C_i(\mathrm{x})$with $i = 1,\ldots,4$ are obtained by a semi-analytic form as shown below.

The constraints $C_i(\mathrm{x})$, with $i = 1,\ldots,4$, depend on **q** that depends on x, and as such:

$$\frac{\partial C_i(\mathrm{x})}{\partial x_i} = \left(\frac{\partial C_i(\mathrm{x})}{\partial \mathrm{q}}\right)^T \frac{\partial \mathrm{q}}{\partial x_i} \tag{52}$$

For the first constraint, we have:

$$\frac{\partial C_1(\mathrm{x})}{\partial x_i} = -\left(\frac{\partial \sigma_c}{\partial \mathrm{q}}\right)^T \frac{\partial \mathrm{q}}{\partial x_i} \tag{53}$$

From the condition of balanced internal and external forces acting on the elements, we have:

$$\mathrm{Kq} = \mathrm{f}_{ext} \tag{54}$$

Considering the external forces as being constant in regards to the design variables and deriving Eq. (54) in relation to x, we have:

$$\mathrm{K}\frac{\partial \mathrm{q}}{\partial x_i} = -\frac{\partial \mathrm{K}}{\partial x_i}\mathrm{q} \tag{55}$$

From Eqs. (54) and (55), we determine **q** and $\frac{\partial \mathrm{q}}{\partial x_i}$: being able then to evaluate $\sigma_c(\mathrm{q})$ and $\sigma_c(\mathrm{q} + \frac{\partial \mathrm{q}}{\partial xi}\Delta q)$, and finally determine that:

$$\frac{\partial \sigma_c}{\partial q_i} = \frac{\sigma_c(\mathrm{q} + \frac{\partial \mathrm{q}}{\partial xi}\Delta q_i) - \sigma_c(\mathrm{q})}{\Delta q_i}$$

5.2. Optimization of the composite section (steel I profile together with the rectangular concrete section)

In this second approach, we intend to determine the dimension of the steel I profile and the rectangular concrete section of the composite steel-concrete beam with partial interaction, so that the cost function related to the steel and concrete volume utilized in the production of this composite element is the minimum possible. Therefore, according to Fig. 9, the objective function can be defined as below:

$$f(\mathrm{x}) = C_S(2b_f t_f + b_w t_w) + C_C l_c h_c \tag{56}$$

Where the vector **x** is given by $\mathrm{x}= \lfloor b_f \;\; t_f \;\; t_w \;\; b_w \;\; l_c \;\; h_c \rfloor$, and C_S and C_C are, respectively, constants that relate the steel and concrete volumes to their production cost.

Similar to the former item, the standard form for the Simplex method for a linearized problem stemming from Eq. (56) is:

$$\min_{\mathrm{d}^*} [\nabla^T f_k \;\; -\nabla^T f_k \;\; 0_{1\times 22}] \mathrm{d}^*$$

Subject to

$$\begin{bmatrix} \nabla^T C_{i,k} & -\nabla^T C_{i,k} & -\mathrm{I}_{20\times 20} & 0 & 0 \\ \nabla^T f_k & -\nabla^T f_k & 0_{1\times 20} & -1 & 0 \\ -\nabla^T f_k & \nabla^T f_k & 0_{1\times 20} & 0 & -1 \end{bmatrix} \mathrm{d}^* = \begin{bmatrix} -C_i(\mathrm{x}_k) \\ -\bar{d} \\ -\bar{d} \end{bmatrix} \tag{57}$$

In the expression above, $\mathrm{d}^* = [\mathrm{d}^{+T} \;\; \mathrm{d}^{-T} \;\; \mathrm{u}^T \;\; \mathrm{w}^T]^T$, where d^+ and d^- are two vectors with 6 components (number of design variables), **u** is a vector with 20 components (number of constraints), **w** is a vector with 2 components (refers to the step size constraint), $\mathbf{I}_{20\mathrm{x}20}$ is an identity matrix of order 20, and $\mathbf{0}_{1\mathrm{x}20}$ is a matrix line with 20 columns of null elements. For greater details as to how to arrive at this standard form, consult Vanderplaats [15]; Haftka and Kamat [16].

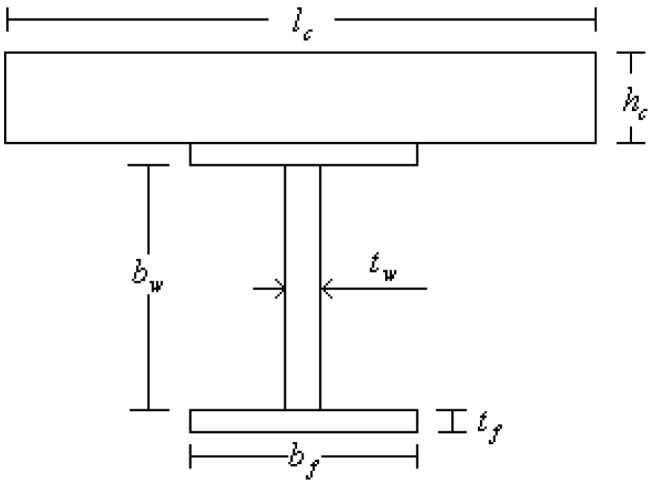

Fig. 9. Composite section.

The derivatives in relation to the objective function and the constraints are obtained in a manner that is analogous to the previous section.

5.3. Optimization of the number of shear connectors

This last approach intends to determine the number of shear connectors needed for a steel-concrete composite beam with partial interaction, so that the number of connectors utilized will be the minimum possible. Thus the objective function can be defined as:

$$f(\mathrm{x}) = \sum_{i=1}^{nc} n_i \tag{58}$$

where n_i is the number of connector along the stretch *i,* and *nc* is the number of stretches into which the beam was divided.

Therefore, as defined in Item 4.3 herein, we have$K = nK_c/\Delta x$, where K is a longitudinal rigidity within the connection, $K_c$is the rigidity modulus of the connector used, and n is the number of equally-spaced connectors along the length of the composite beam. As such, the objective function can be written in function of the connection rigidity and the length of the different stretches of the beam (L_i), so that:

$$f(\mathrm{x}) = \sum_{i=1}^{nc} \frac{L_i}{K_c} K_i \tag{59}$$

In Eq. (59), the vector **x** is given by $\mathrm{x} = \lfloor K_1 \ \ldots \ K_{nc} \rfloor$, while L_i and K_c are specifically determined for each problem depending on the type and configuration of the connector adopted.

Similar to the previous item regarding the standard form for a problem, using Eq. (59) in the Simplex method gives:

$$\min_{\mathrm{d}^*} [\nabla^T f_k \ \ -\nabla^T f_k \ \ 0_{1\times(nr+2)}]\mathrm{d}^*$$

Subject to

$$\begin{bmatrix} \nabla^T C_{i,k} & -\nabla^T C_{i,k} & -\mathrm{I}_{nr\times nr} & 0 & 0 \\ \nabla^T f_k & -\nabla^T f_k & 0_{1\times nr} & -1 & 0 \\ -\nabla^T f_k & \nabla^T f_k & 0_{1\times nr} & 0 & -1 \end{bmatrix} \mathrm{d}^* = \begin{bmatrix} -C_i(\mathrm{x}_k) \\ -\bar{d} \\ -\bar{d} \end{bmatrix} \tag{60}$$

In the above expression, $\mathrm{d}^* = [\mathrm{d}^{+T} \ \ \mathrm{d}^{-T} \ \ \mathrm{u}^T \ \ \mathrm{w}^T]^T$, where d^+ and d^- are two vectors with the number of components given by the number of design variables, **u** is a vector with *nr* (number of constraints) components, **w** is a vector with 2 components (referring to the step size constraint), $\mathbf{I}_{nrxnr}$ is an identity matrix of order *nr*, and $\mathbf{0}_{1xnr}$ is a matrix line with *nr* columns of null elements. For greater details as to how to arrive at this standard form, consult Vanderplaats [15]; Haftka and Kamat [16].

The derivatives in relation to the objective function and the constraints are obtained in a form that is similar to that described in Section 5.1.

6. Examples

6.1. Optimization of the steel I profile – simply supported beam

Aiming to illustrate a practical application for the method developed in this work, the composite beam of Fig. 10 is designed considering both the criteria defined by the Brazilian Code NBR8800 [25] and the method proposed herein.

6.1.1. Design criteria according to Brazilian Standard NBR8800

The load of 150 kN applied to composite beam of Fig. 10 is obtained as a consequence of an ultimate load combination; whereas for serviceability combination, the load of 75 kN is applied for computing the maximum deflection. Consider for the materials in the composite section: f_{ck} = 30 MPa (characteristic concrete strength to compression), f_{yk} = 500 MPa (steel rebar yield strength), $f_{yk} = 250MPa$ (steel beam yield strength) and steel connectors with $f_{yk} = 345\boldsymbol{MPa}$ and $f_{uk} = 415MPa$ (ultimate tensile strength).

6.1.1.1. Pre-dimensioning. For a pre-dimensioning considering the ultimate limit state determinant in the analysis, it is considered total interaction in the steel-concrete connection and the plastic neutral axis (PNA) located at the concrete slab. In this situation the moment of resistance is given by $M_{Rd} = T_{ad}(d_1 + h - 0.5a)$, where $T_{ad} = A_s f_{yd}$ (required Force for the whole cross-section reach the yield stress), $d_1 = d/2$ (half of the total height of the doubly symmetric I profile), h = 12 cm (concrete slab thickness), and a is the distance from the PNA to the upper face of the concrete slab. Given$f_{yd} = f_{yk}/1,10$, M_{Rd} = 375 kNm (maximum moment in the mid-span of the composite beam) and considering a = 9.6 cm (PNA at 80% of the slab thickness), we have $A_s(d + 14.4) = 3300$. Choosing the W310 steel cross-section from the Gerdau table (d approximately 310 mm), we have A_s = 72.7 cm^2, with this area and returning to the Gerdau table we define the profile W310 × 60 (A_s = 76.1, b_w = 277, t_w = 7.5, b_f = 203, t_f = 13.1) as the first attempt to design the composite beam.

6.1.1.2. Connectors for full interaction. Stud-shear connector with 19.1 mm of diameter is adopted in the design. Its design resistance is obtained considering the lowest value between the crushing of the concrete surrounding the connector or the shear rupture of the connector. Since the connectors are welded directly to the profile, and 1.25 is the safety factor adopted to calculate the ultimate resistance of the connector, we have: $Q_{Rd} = 95.12\boldsymbol{kN}$.

The following Eq. (61) quantifies the degree of interaction of the composite beam. In this equation, F_{hd} is the force needed for the plastification of the steel or concrete section, whichever is less. For the chosen section we have F_{hd} = 1729.5kN.

$$\eta = \frac{\sum Q_{Rd}}{F_{hd}} \tag{61}$$

In Eq. (61), $\sum Q_{Rd}$ is the sum of the design ultimate resistances of the connectors arranged between the maximum moment and the adjacent null moment (variable L_e in Eq. (62)). In the case of simply supported beams, L_e corresponds to half length of span. Admitting equally spaced connectors along the span of the beam, the spacing s necessary to have a full shear interaction, that is, $\eta = 1$, is given by the following equation.

$$s = \frac{L_e Q_{Rd}}{F_{hd}} = \frac{5 \times 95.12}{1729.5} = 0,275m \tag{62}$$

The spacing between connectors obtained in Eq. (62) meets the limit values specified by NBR8800 [25]. Dividing the length of the beam by the necessary spacing to have full interaction results in an amount of 37 connectors uniformly spaced along the span of the composite beam.

6.1.1.3. The bending moment resistance. To define the moment resistance of the section it is necessary to check the position of the plastic neutral axis (PNA) in the composite section. For full shear interaction, this position is unique and as $A_s f_{yd} < 0.85 f_{cd} bh$ the PNA is located at the concrete slab at position a = 10 cm below the upper face of the concrete section. In this position, there is an upper rebar and half of the lower rebar is compressed and the other half tensioned, that is, PNA passes through the centroid of the lower rebar.

The moment resistance of the section acting in the centroid of tensioned rebar, when PNA lies in the concrete slab, is given by

$$M_{Rd} = 76.1 \times (25/1.1) \times 0.222 + 6 \times (50/1.15) \times 0.03 = 392.6kNm \tag{63}$$

From Eq. (63), it is observed that $M_{Rd} > M_{Sd}$ and the chosen section in the pre-dimensioning meets the ultimate limit states related to bending. It is considered that the composite beam is laterally restrained so there is no possibility of lateral buckling with torsion, and as the section is all under tension, there are no problems with local buckling of

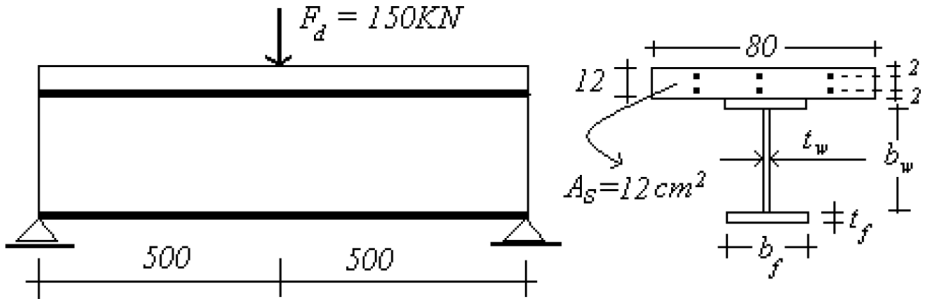

Fig. 10. Simply supported composite beam (dimensions in cm).

the flange or web.

6.1.1.4. Deflection calculation. Linear behavior of the materials is permitted for serviceability load combination. The composite section is transformed into a steel-only section using the homogenization technique employed in the Strength of the Materials, for which the elasticity modules of $E_c = 0.85(5600\sqrt{f_{ck}}) = 26072$MPa for concrete and $E_S = 200000$MPa for the steel section were considered.

Initially, the position of the elastic neutral axis (ENA) is calculated by checking whether it lies within the concrete slab or the steel profile. It is verified that the ENA lies in the steel profile and, therefore, the concrete slab is completely compressed for external actions that do not induce the plastification of the section. The moment of beginning of plastification is the smallest moment between the plastification moments of the most compressed and the most stretched fiber of the section, that is, 188.9kNm. As the maximum moment acting for serviceability combination is less than the moment when plastification begins, it is concluded that the section inertia is constant along the composite beam and given by I = 23523.6 cm^4.

The maximum deflection for a simply supported beam with a concentrated load in the mid- span and constant inertia along the axis is given by the following equation.

$$\delta = \frac{PL^3}{48EI} = \frac{75 \times 1000^3}{48 \times 20000 \times 23523.6} = 3.32cm \tag{64}$$

As the above deflection is larger than the limit deflection of L/350 (2.86 cm), it is verified that the section initially defined does not meet the serviceability limit state of maximum deflection. Therefore, a counter-deflection would be necessary to meet this serviceability limit state.

6.1.2. Proposed method in the present work

A linear stress-strain relationship of the materials is considered in the proposed method of this work. Thus, it is used in the pre-dimensioning of the composite beam in such way to select the steel profile more optimally and then the prescriptions of standards are checked referring to the ultimate limit states.

6.1.2.1. Pre-dimensioning. In the numerical analysis, a mesh of 20 interface elements was adopted for a deformable connection and 40 beam elements, being 20 of the elements for the concrete section and 20 elements for the steel section. The data referring to the physical properties of the materials in the composite section are the same as in the previous item.

According to item 6.1.1.2 of this example, 37 stud-shear connectors with 19 mm of diameter ($F_{max} = Q_{RD} = 95.12$kN) spaced of 27 cm along the span of the composite beam are adopted. Therefore, according to Item 4.3, the stiffness per connector is given by $K_c = 46184$N/mm and the stiffness of the connection per unit length is given by $K = 171.05$MPa.

As described in Section 4.6 herein, some dimension limits were admitted as constraints, and these are:

$\bar{t}_i = 5mm$ (minimum thickness of the flanges and web steel profile)

$\bar{t}_s = 25, 4mm$ (maximum thickness of the flanges and web steel profile)

$\bar{h} = 35cm$ (maximum height of the steel profile)

$\bar{b}_s = 70cm$ (maximum width of the flanges and web steel profile)

$\bar{b}_i = 5cm$ (minimum width of the flanges and web steel profile)

As the structural analysis of the composite beam in this proposed model is based on the linear relationship between stress and deformation of the materials, it is not possible to achieve the total plastification of the composite section, but only the beginning of the plastification. Thus, the use of the load related to an ultimate combination of actions makes the proposed model provides overestimated sections, so the authors suggest that for the verification of the ultimate limit states, 75% of the load related to these limit states should be used when the

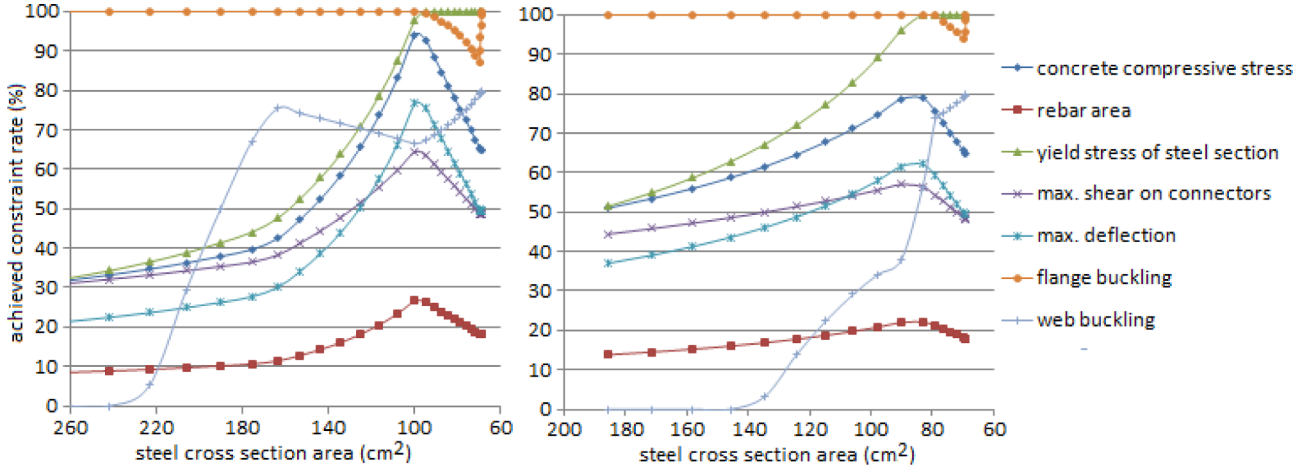

Fig. 11. Evolution of the incremental process.

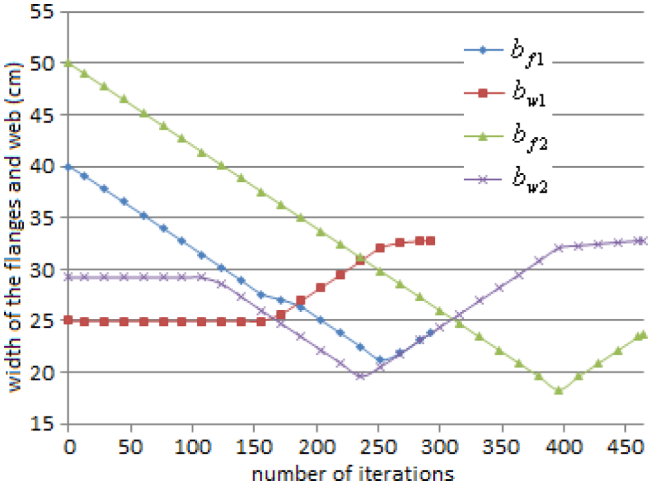

Fig. 12. Evolution of the design variables in the incremental process.

composite beam is not subject to negative moment.

Fig. 11 shows the evolution of the incremental process for solving the nonlinear problem. The graph in the figure depicts how much of the restrictions have already been required with the area of the steel profile at each step of evolution of the incremental process in searching for the optimum point, that is, the steel section of the smallest area that meets all constraints. Fig. 12 shows two graphs for the same problem, the difference being the starting point (as can be seen in Fig. 12), verifying that both converge to a minimum profile area of approximately 68 cm^2.

In Fig. 11, notice that the determinant constraints are those referring to the buckling of the web and the yield stress of the steel profile and there is a gap of approximately 51% in relation to the maximum deflection, 35% in relation to the compression stress in the concrete, 20% in relation to the buckling of the web, 82% in relation to the reinforcement and 52% in relation to the shear of the connectors.

Figs. 12 and 13 show the variation of the design variables along the incremental process evolution in search of the optimum point. The graphs for these figures are compared to the evolution of the search for the optimum point for two distinct starting points.

In the figures below, 1 and 2 used as labels to the design variables, refer to the different starting points adopted. Observe that the convergence for the same cross section is independent of the starting section.

The section A_s = 68.74 cm^2, b_w = 32.79 cm, t_w = 0.5 cm, b_f = 23.72 cm and t_f = 1.10 cm obtained in this section using the proposed method in this work is checked in the following items

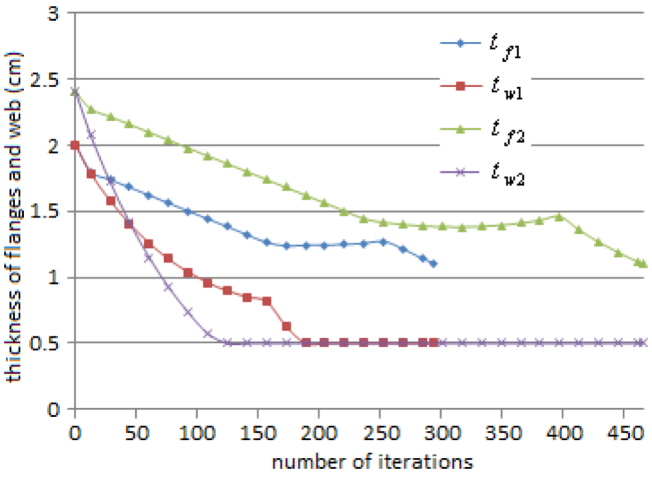

Fig. 13. Evolution of the design variables in the incremental process.

regarding the design criteria stated by NBR8800 for steel–concrete composite beams design.

6.1.2.2. Verification of the optimized section – bending moment resistance. In order to define the resistant moment of the section, it is necessary to verify if for the analyzed section with the distribution of connectors defined in 6.1.2.1 there is full or partial shear interaction of the connection. Since $A_s f_{yd}$ = 1562.3kN is less than the shear force generated by the connectors distributed between the point of null moment and the maximum moment (F_{hd} = 1729.5kN), there is full interaction.

For full shear interaction, this position is unique and as$A_s f_{yd} < 0.85 f_{cd}\, bh$, the PNA is located at the concrete slab at position a = 9.09 cm below the upper face of the concrete section. In this position, the upper reinforcement is compressed with part of the lower reinforcement tensioned and part compressed.

The moment resistance of the section, with PNA being within the concrete slab, the upper reinforcement under compression and disregarding the contribution of the lower reinforcement, is given by

$$M_{Rd} = 68.74 \times (25/1.1) \times 0.250 + 6 \times (50/1.15) \times 0.0254 = 397.2kNm \tag{65}$$

From Eq. (65), it is observed that $M_{Rd} > M_{Sd}$ and the chosen section in the pre-dimensioning meets the ultimate limit states related to bending. It is considered that the composite beam is laterally restrained so there is no possibility of lateral buckling with torsion. The local buckling constraints of the flange and web of the implemented model guarantee these ultimate limit states.

6.1.2.3. Verification of the optimized section – deflection calculation. Similarly to 6.1.1.4, it is noticed that the ENA lies in the steel profile and, therefore, the concrete slab is completely compressed for external actions that do not induce the plastification of the section. The moment of beginning of plastification is the smallest moment between the plastification moments of the the most compressed and the most stretched fiber of the section, that is, 295.7 kNm. As the maximum moment acting for serviceability combination is less than the moment when plastification begins, it is concluded that the section inertia is constant along the composite beam and given by I = 42503.08 cm^4.

The maximum deflection for a simply supported beam with a concentrated load in the mid-span and constant inertia along the axis is given by the following equation.

$$\delta = \frac{PL^3}{48EI} = \frac{75 \times 1000^3}{48 \times 20000 \times 42503.1} = 1.84cm \tag{66}$$

As the above deflection is smaller than the limit deflection of $L/350$ (2.86 cm), it can be seen that the section initially defined also meets the serviceability limit state of maximum deflection.

6.1.3. Comparison between the two solutions

The solution obtained considering the section defined by the proposed model presented a considerable slack in relation to the serviceability limit state of maximum deflection and a plastification moment resistance superior to the soliciting moment obtained for the ultimate loading.

The section defined without the use of the presented algorithm is 10.7% heavier and requires a counter-deflection during its execution to meet the serviceability limit state of maximum deflection.

Using the response of the proposed model to define a practical steel cross-section from the Gerdau table, the authors suggest checking the profile W310 × 52 (A_s = 67, b_w = 317, t_w = 7.6, b_f = 167, t_f = 13.2).

In this example, the increase in the maximum height limit of the profile makes the model present much lighter solutions. For instance, if this limit is changed from 35 cm to 50 cm and the rest of the parameters are maintained, the model provides the profile given by A_s = 53.92 cm^2, b_w = 48.26 cm, t_w = 0.5 cm, b_f = 17.12 cm and

t_f = 0.87 cm. However, in practical terms (for example, using the Gerdau's profile table) it is not possible to have a profile approximately 480 mm height and an area of 53.92 cm^2. A profile with such height has an area of around 100 cm^2, making this solution unfeasible.

6.2. Optimization of the steel I profile – fixed-fixed beam

This example is identical to the previous one, changing only the support conditions at the beam extremities and the number of connectors used.

6.2.1. Pre-dimensioning

In this example, stud-shear connectors of 19 mm diameter (K_c = 46184 N/mm, F_{max} = Q_{Rd} = 95.12 kN) are used spaced with the minimum distance allowed by Brazilian standard (6 times the diameter of the connector). Therefore, according to Item 4.3, the connection stiffness per unit of length is given by K = 405.12MPa. All other data needed to analyze this example is the same as in the previous one.

As in the previous example, the use of the load referring to an ultimate combination of actions causes the proposed model to provide overestimated sections, so the authors suggest that for the verification of the ultimate limit states, 85% of the ultimate load combination should be used when the composite beam is subjected to negative moments.

Fig. 14 (analogous to the previous example) shows two graphs for the same problem, the difference being the starting point (see Figs. 15 and 16), verifying that both converge at a minimum area of approximately 45 cm^2 for the profile. Also observe that in this figure, the preponderant constraints, unlike the previous case, are the constraints related to the flange buckling and the yield stress of the steel profile, with a slack of approximately 78% in relation to beam's maximum deflection, 40% in relation to the compression stress in the concrete, 20% in relation to the buckling of the web, 28% in relation to the yield strength of the reinforcement and 77% in relation to the shear in the connectors.

Observe that in the Figs. 15 and 16, the convergence for the same cross section is independent of the section's starting point.

Then the section A_s = 45.42 cm^2, b_w = 334 mm, t_w = 5 mm, b_f = 176 mm and t_f = 8.2 mm obtained in this example using the proposed method is checked according to the design criteria stated by NBR8800.

6.2.2. Negative bending moment resistance

In order to define the moment resistance of the section, it is necessary to verify if for the analyzed section and the defined connector distribution there is full or partial shear interaction of the connection. Since $A_s f_{yd}$ = 1032.3kN is less than the shear force generated by the connectors distributed between the point of null moment and the maximum negative moment (21 connectors, F_{hd} = 1997kN), there is full interaction.

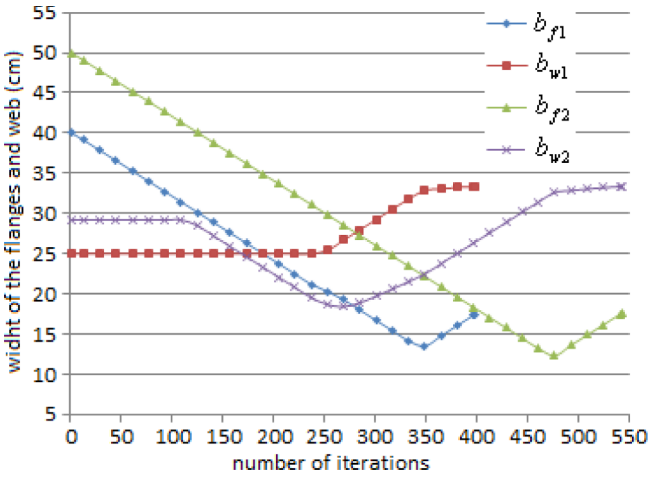

Fig. 15. Evolution of the design variables in the incremental process.

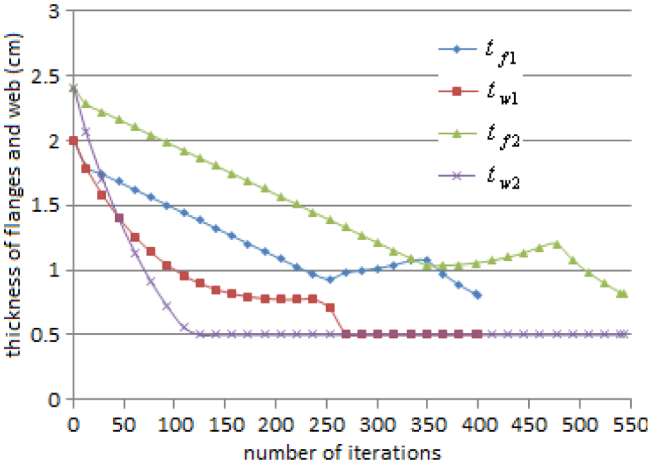

Fig. 16. Evolution of the design variables in the incremental process.

For full interaction the position of the plastic neutral axis (PNA) in the composite section is unique and as $A_s f_{yd} > A_{sb} f_{ybd}$, the PNA is located at the concrete slab at position 0.638 cm below the upper face of the steel profile.

The negative bending moment resistance of the section with PNA within the upper flange of the steel profile is given by

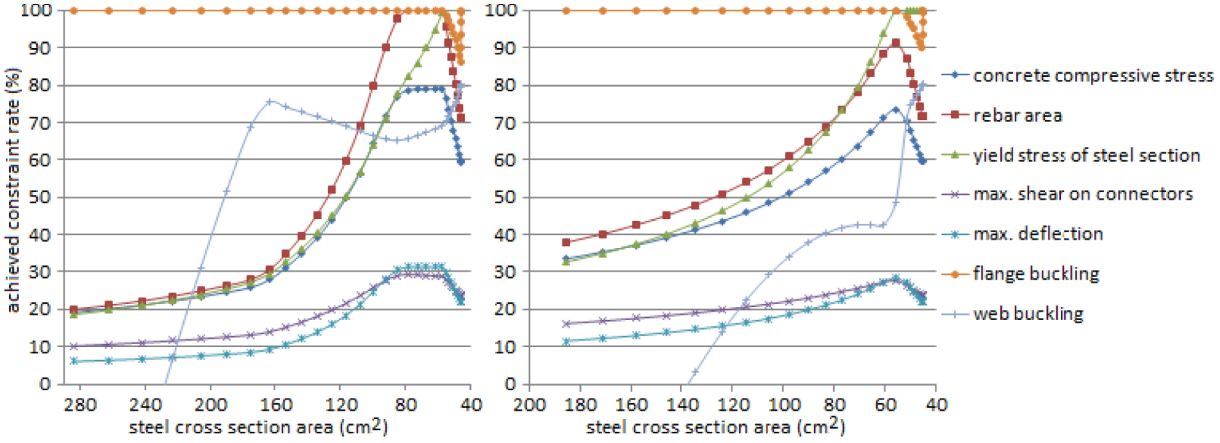

Fig. 14. Evolution of the incremental process.

Table 1
Optimum point for different cost relationships.

Cost: (C_s/C_c)	b_f (cm)	t_f (cm)	t_w (cm)	b_w (cm)	l_c (cm)	h_c (cm)	A_s (cm^2)	A_c (cm^2)
2	25.16	1.43	0.50	26.80	55.16	8.00	85.38	441.28
50	24.68	1.24	0.50	27.27	54.68	16.00	74.77	874.88
100	19.35	1.13	0.50	32.74	58.33	20.00	60.02	1166.61
300	18.90	1.06	0.50	32.87	76.25	20.00	56.65	1524.99

$$M_{Rd} = 5.217 \times (6 + 0.638 + 22.6) + 2.552 \times (0.638/2 + 22.6) = 211kNm \quad (67)$$

From Eq. (67), it is observed that $M_{Rd} > M_{Sd}$ and the chosen section in the pre-dimensioning meets the ultimate limit states related to bending. It is considered that the composite beam is laterally restrained so there is no possibility of lateral buckling with torsion. The local buckling constraints of the flange and web of the implemented model guarantee these ultimate limit states.

6.2.3. Positive bending moment resistance

The positive moment resistance is calculated taking into account the contribution of the concrete, therefore resulting greater than the negative moment resistance, and consequently for the analyzed example, also greater than the solicitant maximum positive moment.

6.2.4. Deflection calculation

For the region of negative moment, disregarding the contribution of concrete, it is noticed that the ENA lies in the steel profile and, therefore, the concrete slab is all tensioned and should really be disregarded in the analysis. The moment of beginning of plastification is the smallest moment between the plastification moments of the most compressed and the most stretched fiber of the section, that is, 153.3 kNm. As the solicitant maximum moment for serviceability loading is less than the moment of beginning of plastification, it is concluded that the section inertia is constant in the negative moment stretch of the composite beam and given by $I = 15255.1$ cm^4.

The maximum deflection for a fixed–fixed beam with a concentrated load in the mid-span and constant inertia along the axis is given by the following equation. As the inertia in the positive moment stretch is greater than the inertia in the negative stretch, it was admitted, in the below equation, constant inertia and equal to the inertia to the negative stretch.

$$\delta = \frac{PL^3}{192EI} = \frac{75 \times 1000^3}{192 \times 20000 \times 15255.1} = 1.28cm \quad (68)$$

As the above deflection is smaller than the limit deflection of $L/350$ (2.86 cm), it can be seen that the section initially defined also meets the serviceability limit state of maximum deflection.

6.3. Optimization of the composite section

In this example, it is shown that the proposed model can also be used for the pre-dimensioning of composite sections. The same beam in Fig. 10 of the previous example was analyzed considering now the objective function given by Eq. (56) and the height and width of the concrete section added to the design variables of the previous example. As the section is composed of two materials, the objective of simply minimizing the sum of the cross-sectional areas of each material would be prioritized for the reduction of the material variables that have a greater area, which generally is the concrete section. To avoid this, we used an objective function given by Eq. (56). This pre-dimensioning section was defined for 4 fictional relationships for the production cost of the structural element: the cost of steel being twice that of the concrete ($C_S = 2C_c$); the cost of steel being 50 times greater than that of the concrete ($C_S = 50C_c$); the steel cost being 100 times more than that of the concrete ($C_S = 100C_c$); and the cost of the steel being 300 times greater than the cost of concrete ($C_S = 300C_c$).

As described in Section 4.6 of this work, some limitations of dimensions were admitted as design constraints. The constraints regarding the steel section are the same as those used in the previous example, whereas for the concrete section, we have:

$\bar{h_i} = 8cm$ (minimum height of concrete section)
$\bar{h_s} = 20cm$ (maximum height of concrete section)
$\bar{l_s} = 220cm$ (maximum width of concrete section)
$\bar{l_i} = 20cm$ (minimum width of concrete section)

Table 1 shows the design variables for different relationships between the cost of steel and concrete after convergence of the optimization iterative method proposed in this work. As can be observed in Table 1, as the relationship between the cost of steel and concrete increases, there is a reduction of the steel area and an increase in the concrete area, as expected.

Next, the composite section shown in Table 1 is checked for the cost of steel being 50 times greater than that of the concrete. The data for reinforcement and connectors are the same as in example 1 for the simply supported beam.

6.3.1. Bending moment resistance

In order to define the moment resistance of the composite section, it is necessary to verify if for the analyzed composite section and the connector distribution defined in 6.1 there is full or partial interaction of the connection. Since $A_s f_{yd} = 1699.3$kN is less than the shear force generated by the connectors distributed between the point of null moment and the maximum moment, ($F_{hd} = 1729.5$kN), there is full interaction.

For full interaction, the position of the plastic neutral axis (PNA) in the composite section is unique and as$A_s f_{yd} < 0.85 f_{cd} bh + A_{sb} f_{ybd}$, the PNA is located at the concrete slab at position $a = 14.4$ cm below the upper face of the concrete section. In this position, the upper reinforcement is compressed with part of the lower reinforcement tensioned and part compressed.

The moment resistance of the section, with PNA being within the concrete slab, the upper reinforcement under compression and disregarding the contribution of the lower reinforcement, is given by

$$M_{Rd} = 74.77 \times (25/1.1) \times 0.237 = 402.3kNm \quad (69)$$

From Eq.(69), it is observed that $M_{Rd} > M_{Sd}$ and the chosen section in the pre-dimensioning meets the ultimate limit states related to bending. It is considered that the composite beam is laterally restrained so there is no possibility of lateral buckling with torsion. The local buckling constraints of the flange and web of the implemented model guarantee these ultimate limit states.

6.3.2. Deflection calculation

It is verified that the ENA lies in the steel profile, therefore the concrete slab is completely compressed for actions that do not plasticize the section. The moment of beginning of plastification is the smallest moment between the plastification moments of the most compressed and the most stretched fiber of the section, that is, 311.8 kNm. As the solicitant maximum moment for serviceability loading is less than the moment of beginning of plastification, it is concluded that the section inertia is constant along the composite beam and given by $I = 39354.7$ cm^4.

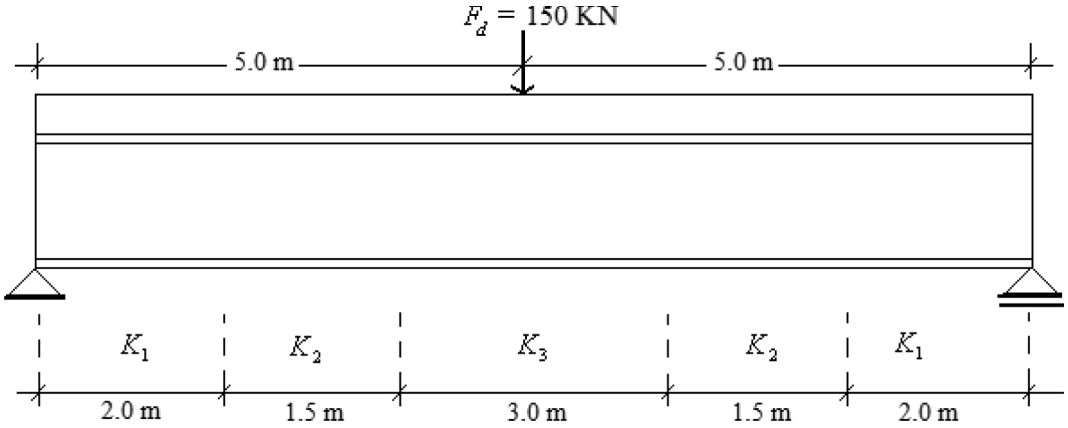

Fig. 17. Stretches with the same longitudinal rigidity in the composite beam connections.

The maximum deflection for a simply supported beam with a concentrated load in the mid-span and constant inertia along the axis is given by the following equation.

$$\delta = \frac{PL^3}{48EI} = \frac{75 \times 1000^3}{48 \times 20000 \times 39354.7} = 1.98cm \tag{70}$$

As the above deflection is smaller than the limit deflection of $L/350$ (2.86 cm), it can be seen that the section defined by the proposed model also meets the serviceability limit state of maximum deflection.

The section obtained in this example compared to the section defined in (6.1) has a higher moment resistance and less deflection, even with a reduction of the section of 8.9% in concrete and 1.7% in steel.

6.4. Optimization of the number of shear connectors – simply supported beam

In this example, the proposed model is used to optimize the distribution of the shear connectors along the simply supported composite beam of Fig. 17, with the cross section given in Fig. 18. The design variables are the longitudinal stiffnesses in the deformable connection. The goal is to searching for the optimum distribution of connectors for a given set of constraints already met.

Fig. 17 shows the configuration adopted for the equally spaced stretches between connectors of the simply supported composite beam analyzed in this example. As can be seen in this Figure, the composite beam was divided into 5 stretches, and as such, due to the symmetry of the problem, there are three design variables, given by the longitudinal rigidity of the deformable connections of the elements of the interface.

As in the previous examples, for the numerical analysis, we used a 20-interface element mesh for the deformable connections, and 40 beam elements, being 20 elements for the concrete section and 20 for the steel section. Therefore, in the first and last stretches of the composite beam of Fig. 18, there will be 4 interface elements that will have a longitudinal rigidity for the connection given by K_1, while the second and the second to the last ones will have 3 interface elements with a longitudinal rigidity for the connection given by K_2, and the middle stretch will have 6 interface elements whose longitudinal rigidity is given by K_3.

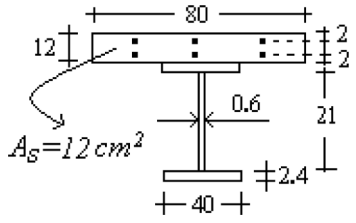

Fig. 18. Cross section (dimensions in cm).

As described in the previous Section 4.7, additions constraints have been admitted for project limitations regarding longitudinal rigidity of the connection. The Brazilian standard NBR-8800 [25] limits the minimum spacing between the connectors to six times the diameter of the connector, and for a 19 mm diameter, we have $e = 0.114m$. While the maximum spacing is limited to eight times the height of the rectangular concrete section of the beam, and for a section height of 12 cm, we have $e = 0.96m$. As seen in Section 4.3, the longitudinal rigidity is given by $K = K_c/e$, then:

$\bar{K_s} = 60874/0.114 = 533982kPa$ (maximum longitudinal rigidity)

$\bar{K_i} = 60874/0.96 = 63410kPa$ (minimum longitudinal rigidity)

Table 2 below displays the design variables after convergence of two different starting points achieved by an iterative method. The composite beam's cross section is shown in Fig. 19. Table 2 also displays the number of connectors needed in each section of the composite beam shown in Fig. 18. It has been verified that this number of connectors increases from the middle to the extremities of the beam, which was expected in the case of the simply supported beams that have null sliding in the middle of the span and maximum sliding at the extremities.

Fig. 19 below demonstrates the evolution of the incremental process for the solution of a non-linear problem. The figure's graph displays how many of the constraints have already been required with the total number of connectors during each step of the evolution of the incremental process in search of the optimum point; in other words, the configuration with the least number of connectors that meets all of the constraints. Observe in Fig. 19 that the maximum deflection constraint is a determinant for the analyzed problem.

Fig. 20 shows the same analysis as that of Fig. 19, only without the maximum deflection constraint. Notice in the figure that the determining constraint changes to the maximum force on the connectors, and that the total number of connectors reduces significantly, going from 57 to 10 connectors (minimum number permitted by NBR-6118 [24].

6.5. Optimization of the shear connector numbers – fixed-fixed beam

This example is analogous to the previous one, changing only the support conditions of the composite beam of Fig. 17, from simply supported to fixed-fixed. Also changing the cross section as shown in Fig. 21.

Table 3 shows the design variables after two different starting points converge using an iterative method. The analysis of cross section of the composite beam is presented in Fig. 22. Table 3 also displays the number of connectors needed for each stretch of the composite beam of Fig. 18, taking into consideration fixed-fixed support.

Fig. 22 below shows the evolution of the incremental process for the solution of a non-linear problem. The graph of the figure relates the

Table 2
Quantity of connectors needed for the section analyzed.

Starting Point			Optimum point			Number of connectors			Total
K_1	K_2	K_3	K_1	K_2	K_3	Stretch 1 and 5	Stretch 2 and 4	Stretch 3	
440,000	533,000	533,000	490,850	440,850	63,140	16	11	3	57
533,000	533,000	150,000	488,529	445,250	63,410	16	11	3	57

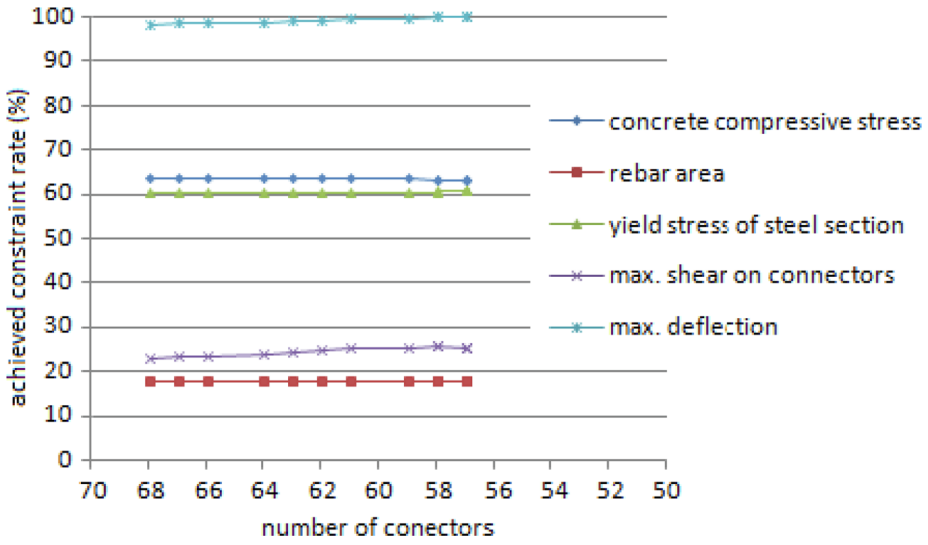

Fig. 19. Evolution of incremental process considering all of the constraints.

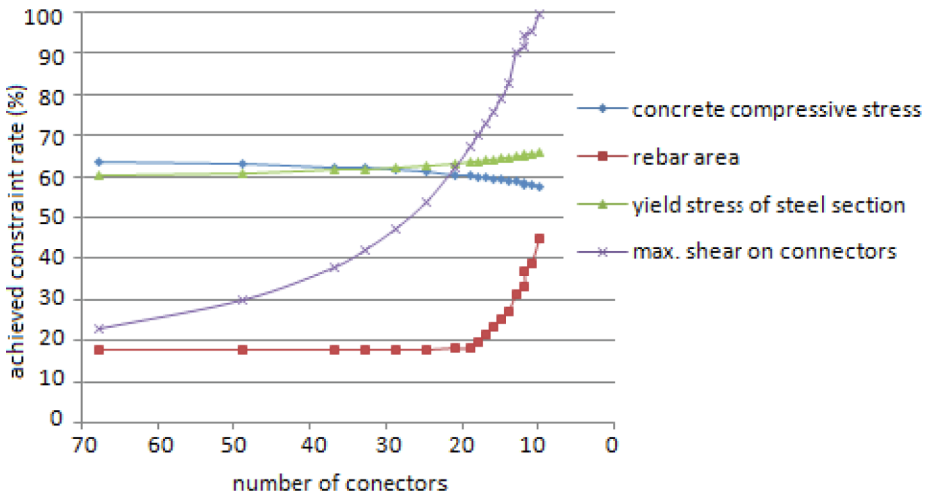

Fig. 20. Evolution of the incremental process without the maximum deflection constraint.

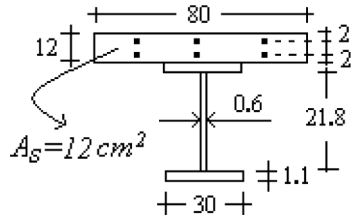

Fig. 21. Cross section (dimensions in cm).

amount of the constraints already required with the total number of connectors for each step of the evolution of the incremental process in search of the optimum point; or in other words, the configuration with the least number of connectors that meets all of the constraints. Observe in Fig. 22 that the maximum deflection constraint together with the initial yield constraint of the steel profile are determinant constraints in the problem analyzed.

Fig. 23 below displays the same analysis as Fig. 22, only without the maximum deflection constraint. Notice is this figure that the determining constraint becomes the maximum force of the connectors, considerably reducing the number of connectors and permitting a gap in relation to the beginning of the yield of the steel profile, which is the determinant for the beam when analyzed with the maximum deflection limited.

7. Conclusions

In this work an optimization algorithm is developed and implemented and coupled with a structural analysis program based on finite element method. The matrix formulation of simplex method is

Table 3
Quantity of connectors need for the analyzed section.

Starting point			Optimum point			Number of connectors			Total
K_1	K_2	K_3	K_1	K_2	K_3	Stretch 1 and 5	Stretch 2 and 4	Stretch 3	
533,000	533,000	533,000	217,340	434,658	307,312	7	11	15	51
250,000	533,000	350,000	208,240	449,642	320,563	7	11	15	51

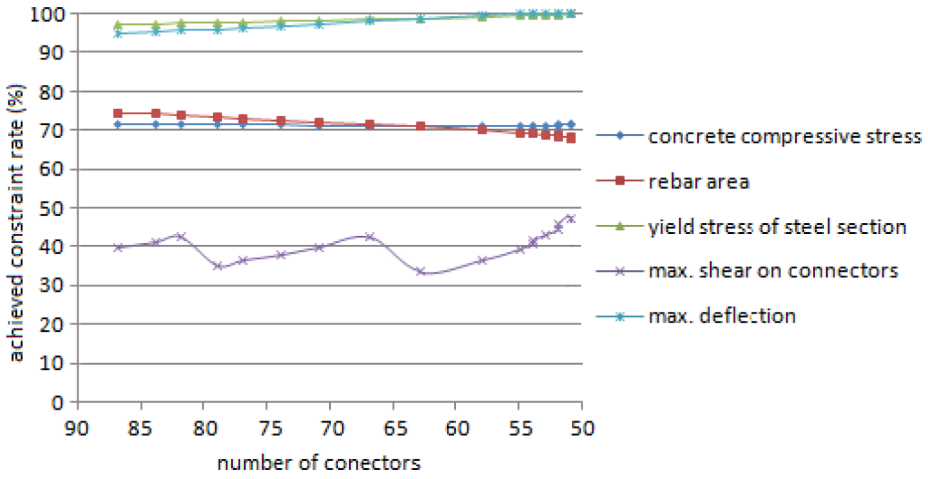

Fig. 22. Evolution of the incremental process considering all of the constraints.

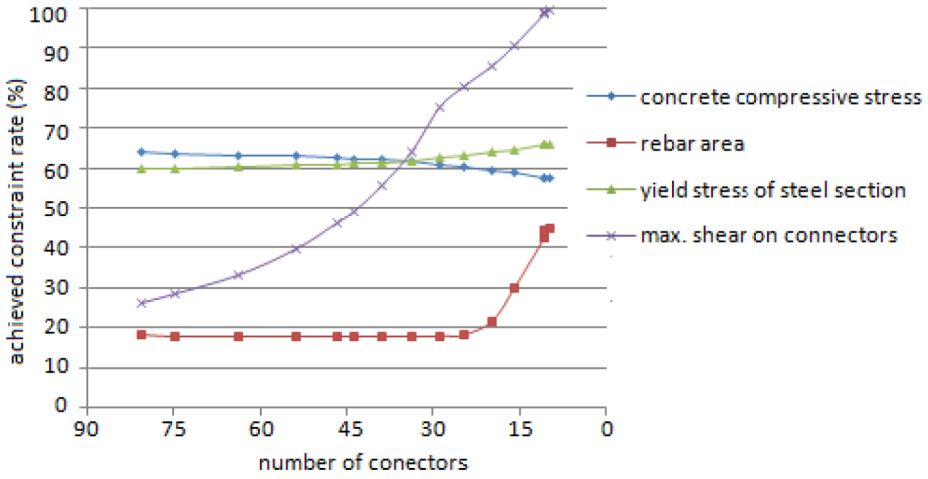

Fig. 23. Evolution of the incremental process without the maximum deflection constraint.

addressed to the nonlinear optimization problem, named sequential linear programming. In numerical modeling of the composite beam, the concrete slab and steel I beam is simulated by one-dimensional beam element, while the deformable shear connection by a one-dimensional interface element. A set of design variables and constraint are taken into consideration. Design variables are considered on different approaches: for the first approach, the dimensions of the steel I profile are only the design variables, remaining to the engineer specify the dimensions of concrete slab and rebar area. In the second approach, the dimension of the steel I profile, along with those of the concrete slab are considered as design variables. And finally, the connector stiffnesses of the deformable connection is considered to be a design variable. Although the followed specifications are according to Brazilian standards, they can be adapted in a straightforward fashion for other, as Eurocode.

As can be observed from the examples presented, the Simplex algorithm used for sequential linear programming problem worked satisfactorily in the optimization of the composite beams when considering different design variables, as well as different constraints and support conditions for a steel-concrete composite beam. In this study, we did not distinguish between the different types of load combinations for the different dimensioning criteria. The dimensioning standards for reinforced concrete and steel (NBR-6118 [24], NBR-8800 [25]) admit different load combinations for verification of the serviceability and ultimate limit states. Thus, in some examples herein, the maximum deflection constraint was removed.

It is important to highlight that the way the results are presented, in terms of percentage of the achieved constraint rate, shows very clearly for a given optimization problem, which constraints can be worked on to improve the performance of the structural system regarding the minimization or maximization of a given objective function. The analysis of results show which constraints drive the composite beam optimization process, when it is observed that some constraints are active (100% of the constraint reached), while other constraints are underused.

Regarding the influence of the type of support condition on the

distribution of connectors, it is observed: on one hand, an increase in the number of connectors from end to center on the simply supported beam; on other hand, an increasing from center to end on the beam with fixed ends. This structural behavior is directly connected to the influence of the interface sliding and on the degree of interaction of the composite beam.

More importantly, the optimization process coupled to the partially connected composite beam analysis process goes in the direction of what is currently understood as advanced analysis: “if the engineer employs an analysis method that adequately represents a limit state, then the checks of corresponding specification would not be required”.

Finally, as can be seen in Section 4, the constraints were based on a linear analysis, so the critical section was taken to the beginning of its plasticity. The dimensioning criteria for reinforced concrete, steel or steel-concrete composite structures permit total plasticity of the cross section for the ultimate load combinations, which has motivated the authors to consider the non-linearity of the materials in a future study.

Declaration of Competing Interest

The authors declare that they have no known competing financial interests or personal relationships that could have appeared to influence the work reported in this paper.

Acknowledgements

The authors thank to CAPES and CNPQ (Federal Research Agencies), FAPEMIG (Minas Gerais State Research Agency) and UFOP for the financial support.

References

[1] Nie J, Fan J, Cai CS. Stiffness and Deflection of Steel-Concrete Composite Beams under Negative Bending. J. Struct. Eng. 2004;130(11):1842–51.
[2] Eskandari Hamid, Korouzhdeh Tahereh. Cost optimization and sensitivity analysis of composite beams. Civil Eng. J. 2016;2(2).
[3] García-Segura Tatiana, Yepes Víctor, Martí José V, Alcalá Julián. Optimization of concrete I-beams using a new hybrid glowworm swarm algorithm. Latin Am. J. Solids Struct. 2014;11:1190–205.
[4] Kravanja S, Z˘ula T, Klanšek U. Multi-parametric MINLP optimization study of a composite I beam floor system. Eng. Struct. 2017;130:316–35.
[5] Papavasileiou Georgios S, Charmpis Dimos C. Seismic design optimization of multi–storey steel–concrete composite buildings. Comput. Struct. 2016;170:49–61.
[6] Senouci Ahmed B, Al-Ansari Mohammed S. Cost optimization of composite beams using genetic algorithms. Adv. Eng. Softw. 2009;40(11):1112–8.
[7] Kaveh A, Abadi A Shakouri, Mahmud.. Cost optimization of a composite floor system using an improved harmony search algorithm. J. Constr. Steel Res. 2010;66(5):664–9.
[8] Kaveh A, Ahangaran M. Discrete cost optimization of composite floor system using social harmony search model. Appl. Soft Comput. 2012;12:372–81.
[9] Kravanja S, Z˘ula, T.. Cost optimization of industrial steel building structures. Adv. Eng. Softw. 2010;41:442–50.
[10] Munck Matthias, Sutter Sven, Verbruggen Svetlana, Tysman Tine, Coelho Rajan Filomeno. Multi-objective weight and cost optimization of hybrid composite-concrete beams. Compos. Struct. 2015;134:369–77.
[11] Kravanja S, Silih S. Optimization based comparison between composite I beams and composite trusses. J. Constr. Steel Res. 2003;59:609–25.
[12] Pedro RL, Demarche J, Miguel LFF, Lopez RH. An efficient approach for the optimization of simply supported steel-concrete composite I-girder bridges. Adv. Eng. Softw. 2017;112:31–45.
[13] Silva, A. R, Sousa Jr., J. B. M e Neves, F. A. Otimização do perfil I de aço de vigas mistas aço-concreto com interação parcial. MECOM/CILAMCE, 2010, Buenos Aires.
[14] Nocedal J, Wright S. Numerical Optimization. second ed. Springer; 2006.
[15] Vanderplaats G. Numerical Optimization Technique for Engineering Design – with Applications. New York: McGraw-Hill Book Company; 1984.
[16] Haftka, R. e Kamat, M. Elements of structural optimization. Martinus Nijhoff Publishers, Boston, 1985.
[17] Bazaraa M, Shetty C. Nonlinear Programming – Theory and Algorithms. second ed. New York: John Wiley & Sons Inc; 1993.
[18] Sousa Jr. JBM, Silva AR. Nonlinear analysis of partially connected composite beams using interface elements. Finite Elem. Anal. Des. 2007;43:954–64.
[19] Sousa Jr. João Batista M, da Silva Amilton R. Analytical and numerical analysis of multilayered beams with interlayer slip. Eng. Struct. 2010;32:1671–80.
[20] Sousa Jr. João Batista M, Oliveira Claudio EM, da Silva Amilton R. Displacement-based nonlinear finite element analysis of composite beam columns with partial interaction. J. Constr. Steel Res. 2010;66:772–9.
[21] Da Silva A, Sousa Jr. JBM. A family of interface elements for the analysis of composite beams with interlayer slip. Finite Elem. Anal. Des. 2009;45:305–14.
[22] Sousa Jr. João Batista M. Exact finite elements for multilayered composite beam-columns with partial interaction. Comput. Struct. 2013;123:48–57.
[23] Machado WG, Neves FA, Sousa Jr. JBM. Parametric modal dynamic analysis of steel-concrete composite beams with deformable shear connection. Latin Am. J. Solids Struct. 2017;14:335–56.
[24] NBR-6118. Projeto de estruturas de concreto – procedimento. Associação brasileira de normas técnicas, 2006.
[25] NBR-8800. Projeto e execução de estruturas de aço e de estruturas mistas aço e concreto de edifícios. Associação brasileira de normas técnicas, 2008.
[26] Oehlers D, Coughlan C. The shear stiffness of stud shear connections in composite beams. J. Constr. Steel Res. 1986;6(4):273–84.